Global Biogeochemical Cycles

RESEARCH ARTICLE
10.1029/2023GB007842

Impacts of Vertical Migrants on Biogeochemistry in an Earth System Model

Julia Getzlaff[1] and **Iris Kriest**[1]

[1]GEOMAR, Kiel, Germany

Key Points:

- We present a global model that represents the impact of mesopelagic fish and vertically migrating organisms on the biogeochemical cycles
- The simulated redistribution of nutrients by vertical migration results in a reduction of the global net primary production by 14%–21% compared to the simulation without vertical migration
- The active carbon export out of the surface layers by vertical migration amounts to ∼25% of the total transport (∼30% of the passive sinking)

Correspondence to:
J. Getzlaff,
jgetzlaff@geomar.de

Citation:
Getzlaff, J., & Kriest, I. (2024). Impacts of vertical migrants on biogeochemistry in an Earth system model. *Global Biogeochemical Cycles*, *38*, e2023GB007842. https://doi.org/10.1029/2023GB007842

Received 11 MAY 2023
Accepted 10 JUL 2024

Author Contributions:
Conceptualization: Julia Getzlaff
Formal analysis: Julia Getzlaff, Iris Kriest
Methodology: Julia Getzlaff
Writing – original draft: Julia Getzlaff, Iris Kriest

Abstract Vertical migrants are a diverse group of organisms, which includes crustaceans, cephalopods and mesopelagic fishes. They play an active role in the biogeochemical cycles but are in general not included in numerical models. In this study we introduce a fully coupled Earth system model that represents vertical migration and with this resolves the key components of the mesopelagic ecosystem, namely migrating zooplankton and mesopelagic fish, including their feedbacks on biogeochemical cycles. The redistribution of nutrients in the water column by vertical migration results in a reduction of the net primary production of 14%–21%, as well as in an asymmetric response in the low oxygenated waters in the tropical Pacific (an increase in the northern and a decrease in the southern oxygen minimum zone). On a global scale, we find the active transport of carbon out of the surface layer to be equivalent to ∼25% of the total export (∼30% relative to passive sinking). In the low latitudes, migration results regionally in a reduction of the shallow export by 2%–10% and an increase of the deep carbon export by 6%–15%. In our simulations, mesopelagic fish, with a biomass of 3–3.4 Gt wet weight, have a slightly larger impact on active carbon flux than migrating zooplankton.

1. Introduction

The ocean twilight zone or mesopelagic (200–1,000 m depth) hosts a diverse community (crustaceans, cephalopods, fishes) and is home to the largest and least exploited fish stocks (see St. John et al., 2016). Many of these organisms perform diel vertical migration (DVM) (Klevjer et al., 2016; McLaren, 1963) to combine both the search for food and the avoidance of predators. On average, migrating organisms prey in shallower waters and migrate to depth where organic carbon is released by respiration, excretion, or egestion. With this, they determine the active carbon pump (Boyd et al., 2019) and have an impact on biogeochemical cycles (Buesseler & Boyd, 2009). Estimates showed that about 10%–20% of the total carbon flux is actively transported from the surface to the ocean interior (Aumont et al., 2019; Davison et al., 2013).

In the past, attention has mainly been paid to migrating zooplankton (Archibald et al., 2019; Gorgues et al., 2019; Longhurst et al., 1990; Steinberg et al., 2000) and their active contribution to the carbon cycle, while the migration of larger animals such as mesopelagic fish only recently started gaining attention. The combination of high biomass, vertical migration, and their excretion of fast-sinking fecal pellets (Davison et al., 2013; Klevjer et al., 2016) is of potential importance for the carbon cycle. In a game-theoretic food web model, Pinti et al. (2023) shows that mesopelagic fish and multicellular zooplankton contribute to more than 50% of the deep carbon sequestration with a sequestration time scale of 250 years that is longer compared to that of other components of the biological carbon pump.

Although biomass estimates of mesopelagic fish are not well constrained and range from early estimates of 1 Gt (Gjøsæter & Kawaguchi, 1980) to more recent estimates of ∼10 Gt (Irigoien et al., 2014), these estimated are close or even larger than estimates of the epipelagic fish biomass (Bar-On et al., 2018; Bianchi et al., 2021). With ongoing fisheries in the upper layers and a decline in epipelagic fish stocks (Galbraith et al., 2017; Lotze & Worm, 2009; Myers & Worm, 2003), there is increasing economic interest in this deeper domain to obtain fish meal to feed aquacultures (Berntssen et al., 2021; Olsen et al., 2020) or as a new and valuable source for proteins (Alvheim et al., 2020), lipids (Wang et al., 2019), minerals and bioactives (Lauritano et al., 2020). Consequences of a potential fishing pressure on this group are largely unknown (e.g., Martin et al., 2020) and are likely to impact the carbon pump and biogeochemical cycles in the epi- and mesopelagic zones.

In general, global models (e.g., all IPCC-type models) insufficiently resolve higher trophic levels, with meso- and/or macrozooplankton being at the top of the model food chain. Mesopelagic processes such as DVM are usually not considered, and the impact of higher trophic levels, such as fish, is only included implicitly by

zooplankton mortality as upper closure term. This upper closure term, however, can have a considerable impact on the biogeochemical model turnover, at regional (Hill Cruz et al., 2021) and global (Getzlaff & Oschlies, 2017) scales.

To date, very few modeling studies have investigated the consequences of DVM for biogeochemical cycling. Bianchi, Stock, et al. (2013) investigated the impact of DVM of zooplankton on biogeochemistry at three 1D stations in the Pacific. Bianchi, Galbraith, et al. (2013) applied an implicit approach (without explicitly modeling DVM) to investigate the impact of DVM on oxygen. Gorgues et al. (2019) assessed the impact of idealized DVM by mesozooplankton on carbon export at different depth horizons. Pinti et al. (2023) investigated global carbon export and sequestration rates mediated by fish and zooplankton in a one-dimensional game-theoretic food web model. Anderson et al. (2019) introduced the first modeling approach that focuses on the mesopelagic. Although their model comprises only five different groups, namely three zooplankton groups (epipelagic, migratory and mesopelagic residence), invertebrates, and mesopelagic fish, it represents the whole mesopelagic ecosystem. While they carried out an extensive sensitivity analysis related to the impact of biogeochemical and biological model parameters, their steady-state flux model did not include any feedbacks of fish on biogeochemical cycles. It also did not resolve the spatial scale, thereby neglecting the impact of different physical-biogeochemical regimes on mesopelagic stocks and turnover, similar to the model by Pinti et al. (2023). To our knowledge, Aumont et al. (2019) present the only model that includes diel vertical migration in a fully coupled end-to-end modeling framework. In their modeling approach, they differentiate between size classes (1 mm–2m) and depth ranges (epipelagic species, migrators and meso-/bathypelagic species) and have in total 64 different groups—a good but computationally expensive approach.

The aim of this study is to present a framework that includes the key components of the mesopelagic ecosystem, namely the impact of migration of zooplankton and mesopelagic fish, in a fully coupled fashion within an Earth system model, while keeping the computational costs as low as possible. For this, we implement the computationally cheap model by Anderson et al. (2019) in a full Earth system model (UVic 2.9). This is a first step to show how the dynamically important mesopelagic ecosystem could be added to IPCC models without losing too much computational efficiency. We systematically show how the mesopelagic ecosystem impacts the nutrient, carbon and oxygen cycles. This study is organized as follows: The model description and the sensitivity simulations are given in Section 2, results are presented in Section 3, followed by a discussion in Section 4 and the conclusions in Section 5.

2. Model Description

2.1. The UVic Earth System Model

We use the University of Victoria Earth system climate model version 2.9 (UVic_ESCM 2.9; hereafter called "UVic") as described in detail by Keller et al. (2012). It comprises a full three-dimensional primitive-equation global ocean model (MOM2, Pacanowski, 1995) coupled to (a) a single-level atmospheric energy-moisture balance model (based on Fanning and Weaver (1996)), (b) a dynamic-thermodynamic sea ice model (Weaver et al., 2001), (c) a simple marine pelagic ecosystem model (Keller et al., 2012), and (d) an active terrestrial vegetation model (Meissner et al., 2003). All model components use a horizontal resolution of 3.6° longitude × 1.8° latitude. The vertical grid of the oceanic component has 19 levels with a thickness of 50 m near the surface, increasing gradually to 500 m in the abyss.

In the ocean model component, isopycnal mixing is parameterized with a globally constant Laplacian isopycnal diffusion coefficient of 1,200 $m^2\ s^{-1}$, and the parameterization by Gent and McWilliams (1990) is applied to include the effect of eddy-induced tracer transport. Below the surface mixed layer, the vertical diffusion coefficient is assumed to be constant in space and time within each simulation. South of 40°S, a value of 1 $cm^2\ s^{-1}$ is added to the background diffusivity in the entire water column to account for observed vigorous mixing in the Southern Ocean (Garabato et al., 2004; Goes et al., 2010). Furthermore, we apply convective adjustment, polar filtering and the tidal mixing parameterization according to Simmons et al. (2004). In all experiments reported here, we use the improved tropical ocean physics as described in Getzlaff and Dietze (2013), where the zonal isopycnal diffusion coefficient is increased by 50,000 $m^2 s^{-1}$ in the equatorial region between 5°S and 5°N in order to mimic the effect of the unresolved equatorial intermediate current system. The wind forcing is prescribed by monthly climatological NCAR/NCEP wind stress fields. Furthermore, we apply preindustrial atmospheric CO_2 conditions (280 ppm) to all simulations.

2.2. The Biogeochemical Component of UVic

UVic features a biogeochemical module that consists of oxygen, two nutrients (nitrate and phosphate), two phytoplankton groups, zooplankton, and sinking detritus (see e.g. Keller et al., 2012). The two phytoplankton components represent diazotrophs and non-nitrogen fixing autotrophs. Both are phosphate-limited, and the latter is additionally limited by nitrate. Iron limitation is simulated with a seasonally varying iron mask to constrain the growth of diazotrophic and non-diazotrophic phytoplankton. The different elements are coupled by a fixed stoichiometry in the organic components.

UVic simulates one generic zooplankton component that grazes on all plankton groups (including itself) and detritus. The simulated zooplankton show the highest abundance in the epipelagic zone due to the high food density in this region, and are nearly absent in the deep waters. Therefore, we consider this type of zooplankton as epipelagic zooplankton Z_e hereafter. Their functional response to food concentration is described by a Holling Type II function, where the grazing preference is 0.3 for phytoplankton, zooplankton and detritus and 0.1 for diazotrophs. The fraction of prey biomass that is converted into zooplankton biomass, respired, excreted or lost to detritus is determined by the growth and assimilation efficiency terms. Zooplankton mortality produces detritus and is described in this model by a quadratic mortality term $\left(m_z \cdot Z_e^2\right)$, where m_z denotes the zooplankton mortality parameter. The remineralization of detritus is temperature dependent. The full model equations, including all sinks and sources, are given in Keller et al. (2012).

2.3. The Mesopelagic Model by Anderson et al. (2019)

Unlike the dynamically varying NPZD-model used in UVic, the model introduced by Anderson et al. (2019) follows a steady-state flux model approach. Apart from estimating mesopelagic fish biomass, no standing stocks are calculated. Here, we provide only a brief overview of the model; all relevant model equations can be found in Appendix A.

The model by Anderson et al. (2019) is forced by net primary production (NPP) as source for zooplankton growth and differentiates between three zooplankton classes: (a) the epipelagic zooplankton (Z_e), (b) vertically migrating zooplankton (Z_m) and (c) detritivorous zooplankton (Z_{Det}) that are permanently resident in the mesopelagic zone. Grazing of epipelagic and migrating zooplankton is a linear function of NPP, whereas grazing of detritivorous zooplankton is determined by export production. Mesopelagic fish feed directly on all three zooplankton groups as well as on invertebrate carnivores, which in turn also graze on the three zooplankton groups. According to the assumptions made by Anderson et al. (2019), invertebrate carnivores represent a variety of organisms such as amphipods, chaetognaths and jellyfish (Daewel et al., 2014; Tönnesson & Tiselius, 2005). Mesopelagic fish biomass is obtained by dividing their growth by their mortality rate, which is in line with the steady-state assumption (Anderson et al., 2019).

2.4. Integrating Mesopelagic Components Into UVic Biogeochemistry

We aim to better resolve possible consequences of mesopelagic processes (particularly DVM) on oxygen, nutrient, and carbon cycles while maintaining the computational feasibility of the Earth system model. In the following, UVic denotes the standard UVic 2.9 model configuration as used, for example, in Getzlaff and Dietze (2013), and UVic-mfish denotes the new model configuration that includes the mesopelagic ecosystem. In addition to the already existing omnivorous epipelagic zooplankton of UVic (Z_e), we introduce of a group of herbivorous, vertically migrating zooplankton (Z_m). Our approach neglects the mesopelagic detritivorous zooplankton considered by Anderson et al. (2019), which contributes only little (6%) to the diet of mesopelagic fish (Anderson et al., 2019).

The conservation equations for Z_e and Z_m including all sinks and sources are given as follows:

$$\frac{dZ_e}{dt} = \omega\, graz_{Ze} - g_{max}\, I_{Ze}\, {Z_e}^2 - m_Z\, Z_e^2 - pred_{Ze}, \quad (1)$$

$$\frac{dZ_m}{dt} = \omega\, graz_{Zm} - m_Z Z_m^2 - pred_{Zm}, \quad (2)$$

where ω denotes the growth efficiency of zooplankton, $graz_{Ze}$ and $graz_{Zm}$ the grazing of Z_e and Z_m, m_Z the mortality parameter, g_{max} the maximum grazing rate, I_{Ze} the ingestion of Z_e by themselves, and $pred_{Ze}$ and $pred_{Zm}$ the fraction of Z_e and Z_m that is ingested by larger mesopelagic animals.

To ensure maximum comparability with the original UVic set-up, we apply the same functional forms for grazing (Holling Type II) to both zooplankton groups. Epipelagic zooplankton in UVic grazes on four different food sources: phytoplankton (P), diazotrophs (D), detritus (Det) and themselves (Z_e). For UVic-mfish, we assume that migrating zooplankton Z_m grazes only on phytoplankton to investigate the behavior of migrating zooplankton solely as competitors of epipelagic zooplankton (and not as their predators). To avoid a too strong grazing pressure on phytoplankton by the extended zooplankton population and to stay as close to the original formulation of UVic as possible, we divide the effective grazing preference for phytoplankton, I_P, by two and apply this adjustment to the grazing of both zooplankton groups (details for this choice are given in Appendix B). Total grazing of epipelagic zooplankton, $graz_{Ze}$, on their four different food sources is then given by

$$graz_{Ze} = g_{max}\, Z_e\, (0.5\, I_P\, P + I_D\, D + I_{Det}\, Det + I_{Ze}\, Z_e). \tag{3}$$

The proportions of grazing on individual food sources (X) are calculated from their relative contribution to total available food:

$$I_x = \frac{p_x}{\sum p_x \cdot X + \kappa_1}, \tag{4}$$

where p_x is the nominal preference for a food source X (either P, D, Det or Z_e), and κ_1 is the half-saturation constant of zooplankton.

In contrast to resident epipelagic zooplankton, migrating zooplankton spends only a fraction of the day (here named τ_Z) in the epipelagic, which is their primary feeding domain. The exact duration of τ_Z depends, among other things, on the latitude: in low and mid latitudes τ_Z aligns with the sun cycle, while Cisewski and Strass (2016) found indications that DVM continues throughout the dark winter period in the high latitudes. Additionally, observational studies have identified a distinct layer of organisms at greater depth during summer, without synchronized vertical movement (Cisewski & Strass, 2016; Conroy et al., 2020). In this unstructured vertical migration the organisms stay in the surface layers until they have fed enough and descend to digest and excrete. Due to this large variability in vertical movement timing, we adopt a first pragmatic approach of setting $\tau_Z = 0.5$, which facilitates direct comparison to the original UVic outcomes. Hence, grazing of migrating herbivorous zooplankton $graz_{Zm}$ is given by

$$graz_{Zm} = \tau_Z\, g_{max}\, Z_m\, 0.5\, I_P\, P \tag{5}$$

We further restrict the grazing by migrating zooplankton to regions where the ocean depth is at least as deep as the migrating depth.

In most global biogeochemical models, including UVic, zooplankton typically represents the highest trophic level, and their mortality is parameterized by a quadratic upper closure term. This term mimics density-dependent losses (e.g., enhanced viral transmission at high organism density) and the impact of predation by higher trophic levels such as epipelagic fish (Mitra et al., 2014; Steele & Henderson, 1992). We maintain this quadratic mortality, denoted as m_Z, with the same constant rate for both zooplankton groups.

In addition to the quadratic mortality, our extended model also resolves the feeding pressure of mesopelagic fish on both zooplankton groups, by applying the same parameterizations as Anderson et al. (2019). Migrating and epipelagic resident copepods provide food to the higher trophic levels of the epipelagic and mesopelagic zones. As no observational estimates exist, Anderson et al. (2019) assume that the fraction of migrating predators to total predators equals the fraction of migrating copepods to total copepods (37%). Assuming migrating predators spend 50% of their time in the epipelagic, this results in an ingestion fraction of epipelagic zooplankton growth of 18%. The food provided by Z_e to mesopelagic fish and invertebrate carnivores is given by:

$$pred_{Ze} = 0.18\, \omega\, graz_{Ze} \tag{6}$$

For the predation of fish and carnivores on migrating zooplankton, Anderson et al. (2019) assume that migrating predators move in a similar manner as their food (synchronized movement). This would result in complete transfer of migrating zooplankton production to migrating predators. However, they also account for the loss of migrating copepods to epipelagic fish during 1 hr at both dusk and dawn (i.e., 2 hr per day). As epipelagic fish are assumed to constitute 63% of total predator biomass, this yields an ingestion fraction of migrating copepod production by epipelagic fish of $0.63 \times 1/24 = 0.052$. The total loss of migrating zooplankton to all predators would be 0.052 + 0.37 (the fraction of migrating predators), and hence the loss of Zm to migrating predators would be given by 0.37/(0.37 + 0.052) = 0.88.

$$\mathrm{pred}_{\mathrm{Zm}} = 0.88\,\omega\,\mathrm{graz}_{\mathrm{Zm}} \tag{7}$$

Similar to Anderson et al. (2019), we do not explicitly represent mesopelagic fish, carnivorous invertebrates, and their vertical distribution, but assume that their growth depends linearly on that of zooplankton (as in the last terms on the right hand side of Equations 1 and 2). Hence, the two groups are only implicitly embedded in the model. We do not prescribe any depth preference for their feeding but assume that these organisms may actively search and hunt for their prey. In the global domain, the growth terms G_V (carnivores) and G_F (fish) of these two components are represented by a two-dimensional component:

$$G_V = \left(1 - f_{Z,F}\right) \cdot K_V \cdot \int \left(\mathrm{pred}_{\mathrm{Zm}} + \mathrm{pred}_{\mathrm{Ze}}\right) \mathrm{d}z, \tag{8}$$

$$G_F = f_{Z,F} K_F \cdot \int \left(\mathrm{pred}_{\mathrm{Zm}} + \mathrm{food}_{\mathrm{Ze}}\right) \mathrm{d}z + f_{V,F} G_V, \tag{9}$$

where K_V denotes the growth efficiency of invertebrate carnivores, K_F that of mesopelagic fish, $f_{Z,F}$ the fraction of zooplankton growth consumed by mesopelagic fish, and $f_{V,F}$ the fraction of carnivore invertebrates consumed by mesopelagic fish.

To obtain estimates of simulated fish biomass B_F, we divide fish growth by an assumed mortality rate in analogy to the approach by Anderson et al. (2019):

$$B_F = G_F \cdot \sigma / m_F, \tag{10}$$

where m_F denotes the mesopelagic fish mortality and the conversion coefficient σ (946.89 g wet weight per mol N, that is 11.9 g wet weight per g C dry weight based on the conversions of 0.2 dry to wet weight and 0.42 for C fraction dry weight (Ikeda et al., 2011)). An overview of all parameters is given in Table 1 and an overview of model state variables is given in Table 2.

Natural mortality is one of the most important parameters characterizing the productivity of fish stocks, and errors in this value can have substantial effects on the resulting fish biomass (Punt et al., 2021). In most methods, fish mortality depends on longevity, although there are large differences in the exact formulation. Anderson et al. (2019) defines the mortality parameter as the inverse of longevity t_{max}, whereas the so called rule-of-thumb approach (e.g., (Hoenig, 1983)) estimates the mortality as $3 \cdot t_{max}^{-1}$, and Then et al. (2014) advocates $4.899 \cdot t_{max}^{-0.916}$. Assuming a longevity for mesopelagic fish of 1.5 years as in Anderson et al. (2019) results in a mortality that ranges between 0.67 and 3.38 year^{-1} depending on the method applied. One advantage of our approach is that the simulated feedback on the biogeochemistry is independent of the mesopelagic fish mortality. In the default model set-up presented here, we adhere to the mortality value of 0.67 year^{-1} as proposed by Anderson et al. (2019), and discuss the impact of this choice in Section 4.

The loss terms of epipelagic and vertically migrating zooplankton lead to the production of nutrients and detritus through excretion, sloppy feeding, egestion of fecal pellets and zooplankton carcasses (see Keller et al., 2012 for more details). For epipelagic zooplankton, this occurs in the same vertical domain as their grazing. However, migrating zooplankton graze in the surface layer but excrete and egest in deeper layers (Bronk & Steinberg, 2008; Steinberg, Cope, et al., 2008; Steinberg, Van Mooy, et al., 2008). To incorporate the process of vertical migration, we instantly redistribute the excreted and egested material to the DVM layer. We adopt a pragmatic approach

Table 1
Overview of All Parameters

Parameter	Definition	Value	Unit
ω	Growth efficiency of zooplankton	0.4	Dimensionless
m_Z	Zooplankton mortality parameter	0.06	$(\text{mmol N/m}^3)^{-1}\ \text{day}^{-1}$
κ_1	Half saturation constant of Z_e	0.15	mmol N m^{-3}
p_p	Preference of Z_e on P	0.3	Dimensionless
p_{Ze}	Preference of Z_e on Z_e	0.3	Dimensionless
p_{Det}	Preference of Z_e on Det	0.3	Dimensionless
p_D	Preference of Z_e on D	0.1	Dimensionless
τ_Z	Fraction of day of Z_m spending in the epipelagial	0.5	Dimensionless
K_V	Growth efficiency of invertebrate carnivores	0.22	Dimensionless
K_F	Growth efficiency of mesopelagic fish	0.2	Dimensionless
$f_{Z,F}$	Fraction of zooplankton growth consumed by mesopelagic fish	0.5	Dimensionless
$f_{V,F}$	Fraction of invertebrate carnivores consumed by mesopelagic fish	0.8	Dimensionless

compared to the regionally varying migration depths approximated by Bianchi, Galbraith, et al. (2013) or Aumont et al. (2019) by assuming a discrete and spatially uniform migration depth. This allows a straightforward testing of the impact of DVM depth on the underlying biogeochemistry by varying the DVM depth in a set of sensitivity simulations.

In analogy to the steady state approach by Anderson et al. (2019), we assume that the ingestion of mesopelagic fish and invertebrate carnivores equals their total losses. In the absence of external sinks such as fishing, these losses will remain in the ocean ecosystem either in dissolved or particulate form. We consider these losses eventually become detritus. The two different depth distributions, D_{F1} and D_{F2} as depicted in Figure 1, of this particular source of detritus are prescribed and applied in the sensitivity simulations described in Section 2.5.

Table 2
Overview of Model State Variables and Fluxes Associated With Higher Trophic Levels

Model variables	Definition
P	Phytoplankton
Z_e	Epipelagic zooplankton
Z_m	Migrating zooplankton
Det	Detritus
D	Diazotrophs
$graz_e$	Grazing of Z_e
$graz_m$	Grazing of Z_m
I_P	The ingestion of Z_e on phytoplankton
I_{Ze}	The ingestion of Z_e by themselves
I_D	The ingestion of Z_e on D
I_{Det}	The ingestion of Z_e in Det
$pred_{Ze}$	Predation of fish and carnivores on Z_e
$pred_{Zm}$	Predation of fish and carnivores on Z_m
G_V	Growth of invertebrate carnivores
G_F	Growth of mesopelagic fish
B_F	Mesopelagic fish biomass

Assuming that all ingested zooplankton is immediately redistributed as detritus by the given vertical function of D_F is a pragmatic choice that ensures mass conservation and allows us to keep the model computationally efficient (only one explicit tracer compartment Z_m is added) while resolving the most important processes (see simplified schematic of the coupled model in Figure 2). Lacking knowledge about the metabolic rates of mesopelagic fish makes it difficult to differentiate between the redistribution in dissolved and particulate material. Therefore, our strong assumption can be interpreted as an upper limit estimate.

When adding a new ecosystem to a biogeochemical model, it is very likely that the model parameters need adjustment. In our case, the structural changes in the ecosystem, along with UVic's default parameters, initially increased the grazing pressure on phytoplankton compared to the original UVic 2.9 set-up. The increased grazing pressure led to a reduction in NPP, particularly in the high productive regions at low latitudes. To regulate NPP in UVic-mfish, we adjusted the phytoplankton mortality parameter, which represents fast (bacterial) remineralization, as well as the maximum grazing rate (at 0°C). Specifically, we reduced the maximum grazing rate from 0.4 to 0.2 day^{-1} and increase the phytoplankton mortality from 0.015 to 0.03 day^{-1}. Additionally, we changed the half-saturation constant for iron limitation of phytoplankton growth from 0.1 to 0.15 nmol Fe m^{-3} and adjusted the detritus remineralization rate from 0.055 to 0.065 day^{-1}. With these changes, we are able to simulate similar NPP distributions in both model configurations.

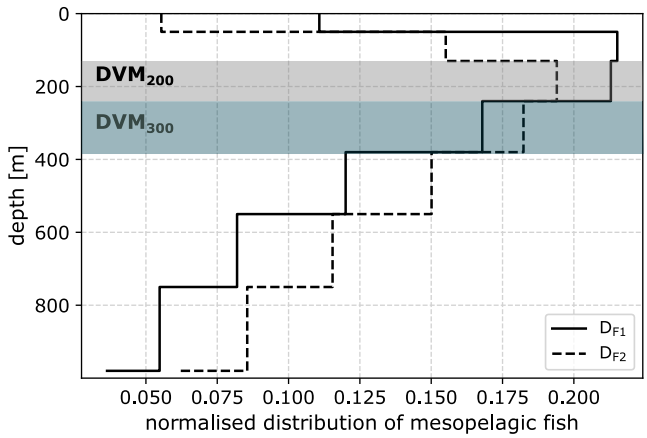

Figure 1. Normalized vertical distribution of mesopelagic fish weighted by the thickness of the respective model layers for two different case studies. The shaded areas show the two migration depth ranges of the migrating zooplankton.

2.5. Sensitivity Simulations

We conducted a series of sensitivity simulations to evaluate the representation of mesopelagic fish and to explore the influence of migratory processes on biogeochemistry. The details of these simulations are outlined below and summarized in Table 3.

UVic: This simulation is the standard UVic 2.9 model configuration (e.g., Getzlaff & Oschlies, 2017; Getzlaff et al., 2016).

noDVM: In this model configuration, we used the fully coupled model UVic-mfish, but without any vertical migration of either zooplankton or fish. By doing so, migrating zooplankton and mesopelagic fish excrete and egest in the same layers as epipelagic zooplankton (close to the surface).

noDVM-F1: In this set-up, assumptions for migrating zooplankton are identical to noDVM, but we assume that the contribution of the mesopelagic fish to detritus production has the globally uniform vertical distribution D_{F1} as shown in Figure 1.

$DVM_{200}F1$: This setup features UVic-mfish, including diel vertical migration by zooplankton as well as the impact of mesopelagic fish on the vertical distribution of detritus. The diel vertical migration depth of zooplankton is set to the depth range between 130 and 240 m (the third vertical model layer) and the contribution of the mesopelagic fish to detritus to the globally uniform vertical distribution D_{F1} as shown in Figure 1.

$DVM_{200}F2$: This set-up is similar to $DVM_{200}F1$ but the contribution of the mesopelagic fish to detritus has the globally uniform vertical distribution D_{F2} as shown in Figure 1.

$DVM_{300}F2$: This simulation is configured in the same way as $DVM_{200}F2$, but with a deeper migration depth of Z_m of 240–380 m (the fourth vertical layer of the model).

An overview of all model simulations is given in Table 3. Each sensitivity simulation was run for 10,000 years until reaching quasi steady-state conditions. For the presentation of the results, we calculate the annual mean of each simulation after 10,000 years. The impact of DVM is then presented as the ensemble mean $\overline{DVM}$ of all simulations that include DVM ($DVM_{200}F1$, $DVM_{200}F2$, $DVM_{300}F2$). The uncertainty within the DVM ensemble that arises from different assumptions about the migration depth is denoted by error bars.

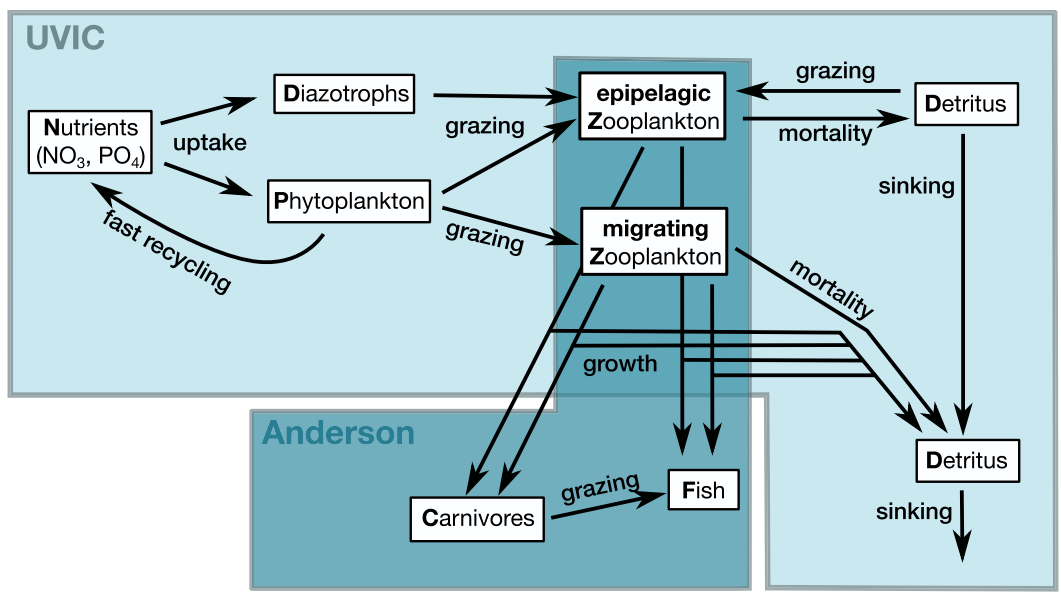

Figure 2. Schematic of integrating the Anderson approach into UVic 2.9.

Table 3
Overview of All Sensitivity Simulations

	UVic	noDVM	noDVM-F1	$DVM_{200}F1$	$DVM_{200}F2$	$DVM_{300}F2$
Max. grazing rate (day^{-1})	0.4	0.2	0.2	0.2	0.2	0.2
Phytoplankton mortality rate (day^{-1})	0.015	0.3	0.3	0.3	0.3	0.3
Half sat. constant for iron limitation (nmol Fe m^{-3})	0.1	0.15	0.15	0.15	0.15	0.15
Detritus remineralization rate (day^{-1})	0.055	0.065	0.065	0.065	0.065	0.065
Z_m	No	Yes	Yes	Yes	Yes	Yes
Z_m migration	No	No	No	130–240 m	130–240 m	240–380 m
Mesop. fish	No	Yes	Yes	Yes	Yes	Yes
Mesop. fish migration	No	No	D_{F1}	D_{F1}	D_{F2}	D_{F2}

3. Results

3.1. Zooplankton

The total zooplankton biomass of 0.5–0.53 Gt C in our simulation (Figure 3, Table C1) is at the upper end of estimates observed by Buitenhuis et al. (2013), but within the very large uncertainty range given by Drago et al. (2022). Furthermore, the distribution of vertically integrated zooplankton biomass in UVic is similar to the vertical integral of the net zooplankton biomass of $DVM_{200}F1$ (Figures C1a and C1b) showing large maxima in the tropical oceans and also large values in the high latitudes. In UVic-mfish, this distribution is mainly determined by Z_e (Figure C1c), while migrating zooplankton shows a rather homogeneous distribution with smaller concentrations in the Southern Ocean (Figure C1d).

Observations comparing day and night measurements of mesozooplankton in surface waters are commonly used to estimate of the proportion of migration zooplankton. The observed fraction of migrators relative to total zooplankton (migrators and non-migrators) exhibits large spatial and seasonal variability. Estimates range between 0.34 and 0.38 for the equatorial Pacific at 140°W (Zhang & Dam, 1997), 0.33–0.71 (depending on season and year, with a mean of 0.38) for the Sargasso Sea (Madin et al., 2001), 0.41 to 0.48 for the subtropical Pacific (Al-Mutairi & Landry, 2001; Steinberg, Cope, et al., 2008; Steinberg, Van Mooy, et al., 2008) and 0.6 for the subarctic Pacific (Steinberg, Cope, et al., 2008; Steinberg, Van Mooy, et al., 2008). Our global and large-scale estimates are at the lower end of these observations but neglect the spatial variability of the model at smaller scales. Figure 4 depicts the spatial distribution of the contribution of migrating to total zooplankton, derived from annual mean concentrations of experiment $DVM_{200}F1$. Although the temporal averaging might reduce some of the potential variability, we also see a large spatial variability with values that are in the range of the observational ones.

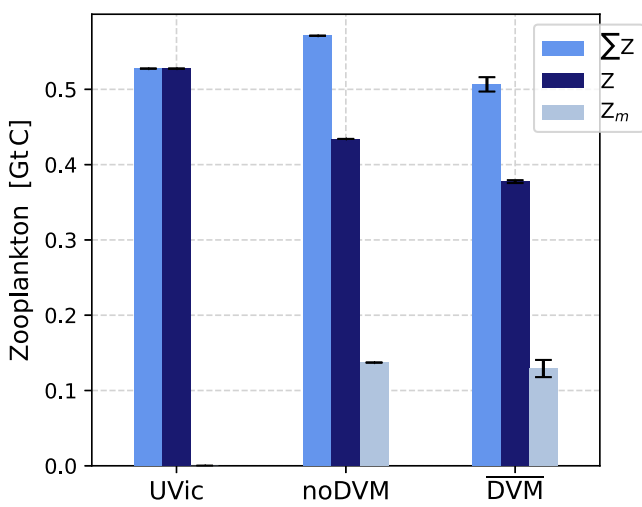

Figure 3. Globally integrated zooplankton biomass.

The relative importance of migrating zooplankton in the tropics and subtropics can be explained with the model's assumptions of epipelagic zooplankton grazing and their diet preferences: Low phytoplankton concentrations in the oligotrophic subtropical gyres limit zooplankton grazing on this resource. Consequently, the omnivorous epipelagic zooplankton Z_e switches to other types of food, including itself, thereby limiting its own growth. This results in lower concentrations (Figure C1, panel c) and, together with the low but homogeneous distribution of strictly herbivorous migrating zooplankton (Figure C1, panel d), contributes to a smaller contribution of Z_e to total zooplankton. In contrast, omnivory of Z_e appears advantageous compared to herbivory in the Southern Ocean, which experiences long periods of nearly absent phytoplankton during austral winter. In this region Z_e constitutes the largest fraction of zooplankton, evidently outcompeting migrating organisms due to their more flexible diet, higher growth rate (due to a longer presence in surface waters) and lower predation by mesopelagic fish (Equations 1 and 2). Thus, while low growth rates and high loss rates of migrating zooplankton contribute to their overall low simulated concentration, the assumed dietary preferences of both groups, along with intra-guild predation of epipelagic

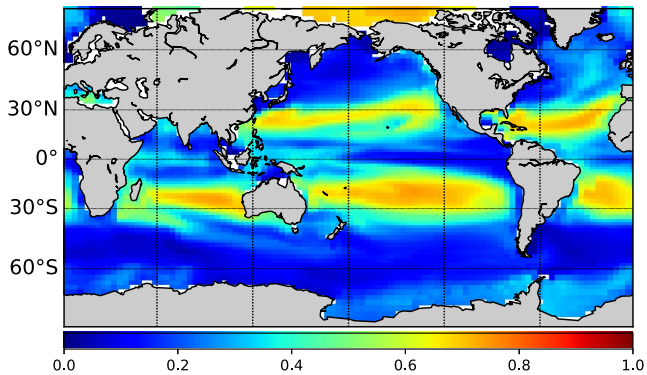

Figure 4. Relation of migrating zooplankton Z_m to total zooplankton ($Z_e + Z_m$) in $DVM_{200}F1$.

zooplankton, cause the large spatial variability in their contribution to total zooplankton.

3.2. Mesopelagic Fish

In contrast to the approach by Anderson et al. (2019), our model incorporates grazing by the mesopelagic fish, which directly impacts the standing stock of zooplankton. Concurrently, fish egestion and mortality affects the production and export of detritus, with potential feedbacks on remineralization and the provision of recycled nutrients for primary production. To investigate the impact of feedbacks induced by the two-way coupling on the resulting mesopelagic fish biomass, we compare the results of UVic-mfish with those obtained by the one-way coupling approach introduced by Anderson et al. (2019) (referred to as A2019 hereafter). For the A2019 (one-way coupled) model, we use primary production from the respective simulations of UVic-mfish as input and employ the default parameters provided by Anderson et al. (2019). Globally integrated mesopelagic fish biomass simulated by UVic-mfish generally exceeds the estimates from A2019 (Figure 5).

Although the distribution pattern of the mesopelagic fish (an example for $DVM_{200}F1$is shown in Figure 6a) appears to align with the pattern of NPP (Figure 6b), the fraction of fish growth attributed to NPP shows large regional differences (Figure 6c). While this fraction remains constant at a value of 0.003 for A2019, UVic-mfish shows a higher fraction in the high productive tropics and in the upwelling region in the Southern Ocean, and a smaller fraction in the Southern Ocean south of ∼50°S and in the less productive regions of the subtropical gyres. This indicates that the response of the fish biomass in the fully coupled model is more sensitive to changes in NPP in the low latitudes (as indicated by the larger fraction between fish growth and NPP) compared to the fish biomass by A2019.

Indeed, this is in line with the differences in the response to vertical migration between UVic-mfish and A2019. Comparing noDVM and $\overline{\text{DVM}}$, the globally integrated mesopelagic fish biomass is reduced by 14%–21% when A2019 is forced with NPP from the respective simulations (Figure 5). This reduction increases to 19%–42% when using the fully coupled approach in UVic-mfish. These results indicate non-linear interactions with the ecosystem dynamics of the lower trophic levels, as variations in the A2019 fish biomass estimates are solely implied by changes in NPP.

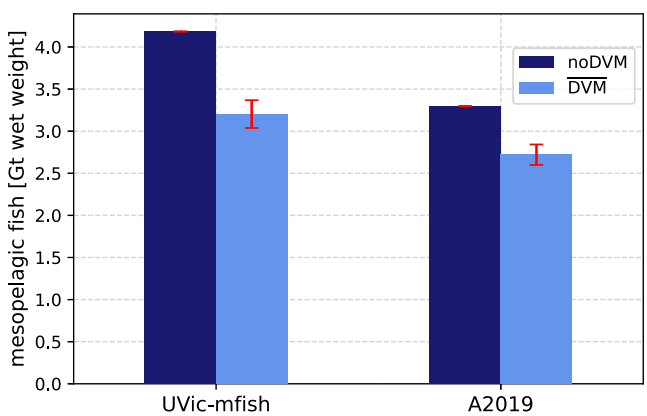

Figure 5. Globally integrated biomass of mesopelagic fish for the 2-way coupled UVic-mfish approach and the linear approach introduced by Anderson et al. (2019) (A2019) with NPP as forcing for noDVM and $\overline{\text{DVM}}$. The error bars indicate the impact of differences in the vertical migration depth.

3.3. Impact on Biogeochemistry

3.3.1. Net Primary Production

In the low latitudes (integrated between 40°S and 40°N), observations show a wide range of estimates for NPP, that are 46.3 Gt C y^{-1} by Behrenfeld and Falkowski (1997), 63.3 Gt C y^{-1} by Carr (2001), and the most up-to-date value of 43.0 Gt C y^{-1} by Westberry et al. (2008). In the default UVic configuration, NPP has a global value of 49.4 Gt C y^{-1} and a value of 36 Gt C y^{-1} integrated between 40°S and 40°N, which is lower compared to observations (Table C2). Simulation noDVM matches the observations with a NPP of 43.3 Gt C y^{-1} between 40°S and 40°N very well and shows the largest NPP of all simulations, whereas the DVM simulations yields an NPP estimate similar to UVic's.

Diel vertical migration by zooplankton as well as mesopelagic fish actively transport detritus to deeper layers (Figure C4), and with this, a fraction of detritus escapes the fast remineralization in the warm waters of the epipelagic zone. This, in turn, impacts the amount of nutrients supplied to the surface layers compared to model configurations that miss migratory processes, and is of particular importance for nutrient limited regions where it affects NPP (see Table C2). The migratory processes of Z_m and mesopelagic fish in

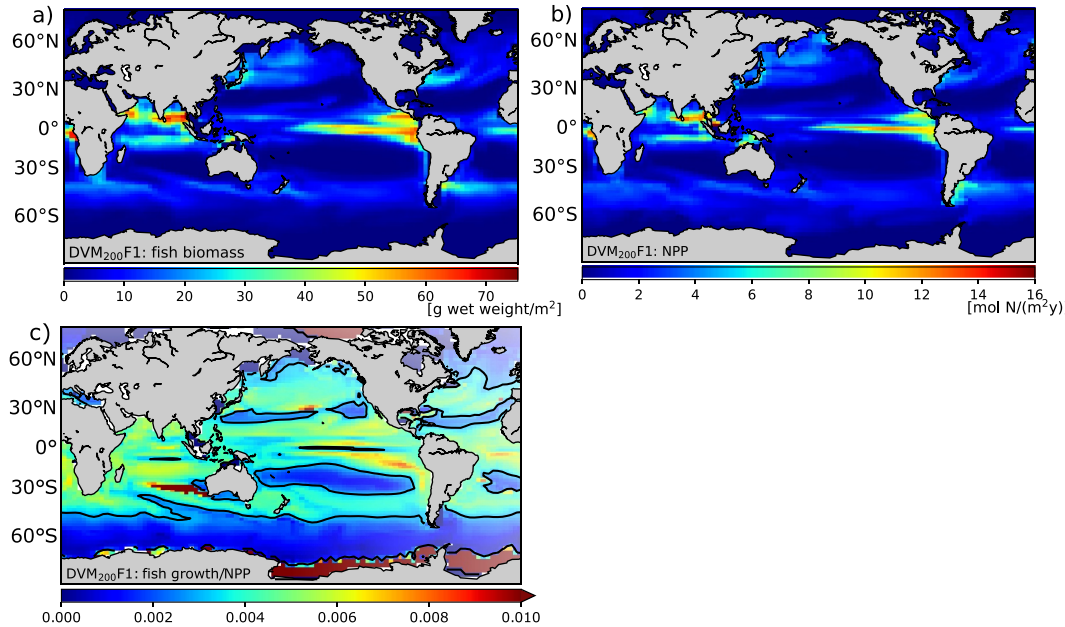

Figure 6. Vertically integrated biomass of mesopelagic fish (a) and vertically integrated net primary production (b) for $DVM_{200}F1$. (c) Relation between growth of mesopelagic fish and NPP in $DVM_{200}F1$. The contour line in indicates the constant value of 0.003, which is the relation between mesopelagic fish growth and NPP for A2019.

scenarios that include vertical migration lead to a reduction of the globally integrated NPP by 9%–21% (Figure 7). The largest reduction (14%–29%) occurs between 40°S and 40°N. This is in line with a strong reduction of NO_3 and PO_4 in the surface layer at low latitudes (Figure 7). In the nutrient replete but light limited Southern Ocean, we find that a small reduction in zooplankton releases the grazing pressure on phytoplankton, leading to the small increase of NPP. The increase in NPP also leads to an increase in surface remineralization and thus a small increase of NO_3 and PO_4 in the surface layer.

3.3.2. Carbon Export

Vertical migration affects also the export of carbon from the surface to the ocean interior. The total carbon export includes all processes that export carbon to depth, including export by sinking particles, active export and mixing. Here, we have to differentiate between carbon export production, which is typically estimated at a depth horizon of ∼100–120 m, and deep carbon export, where export horizons are typically set between 500 and 2,000 m (Guidi et al., 2015; Henson et al., 2012; Jin et al., 2020). We choose three different depth horizons: (a) 125 m to investigate changes in the total export production, (b) 550 m, which is one model layer below the deepest assumed migration depth of Z_m, and (c) 1,500 m, which is below the migratory impact of mesopelagic fish. An overview of all values is given in Table C2, and a comparison with sediment trap data from Mouw et al. (2016) is shown in Figure C2.

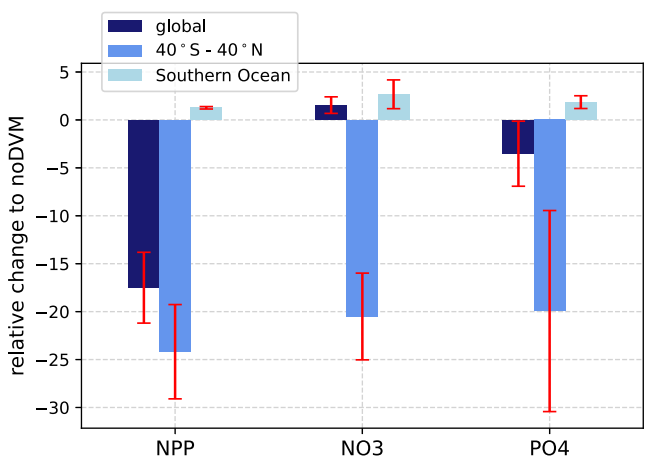

Figure 7. Global (dark blue) and regional (blue: 40°S–40°N; light blue: Southern Ocean) properties (NPP, nitrate and surface phosphate) of $\overline{DVM}$, expressed as percent deviation from noDVM. The error bars indicate the impact of differences in the vertical migration depth.

When investigating the impact of the migratory processes on the total carbon export, we are particularly interested in the impact of migratory processes in UVic-mfish on the total carbon export by comparing noDVM with all sensitivity simulations that include DVM. Figure 8 shows the relative change of the total carbon export for the three sequestration horizons relative to noDVM. As expected from the low NPP, the carbon export at the 125 m depth horizon is smaller for all simulations that include DVM and for all three regions (globally, 40°S–40°N, Southern Ocean) compared to noDVM. This reduction of the total transport at the 125 m depth horizon is partly determined

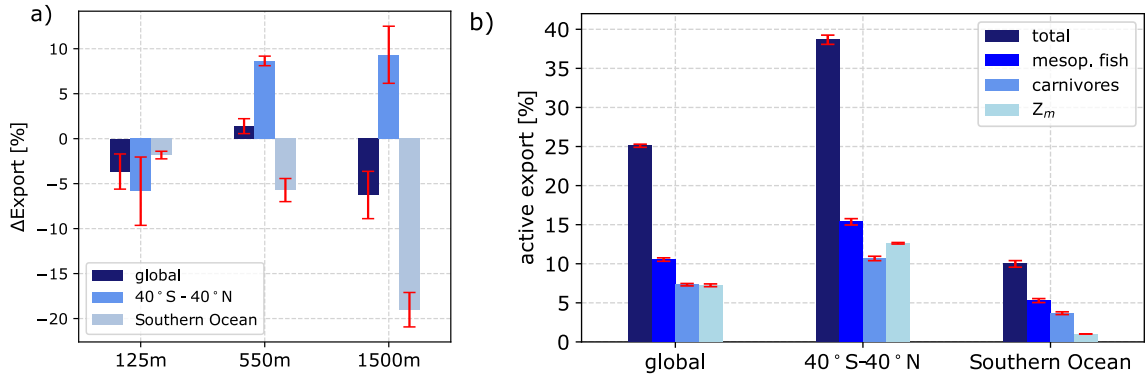

Figure 8. (a) Globally integrated export production (dark blue), export production integrated between 40°S and 40°N (blue), and integrated across the Southern Ocean south of 40°S (light blue) across 125, 550, and 1,500 m for $\overline{\text{DVM}}$ relative to noDVM. (b) Active export for $\overline{\text{DVM}}$ relative to total export at the 125 m depth horizon by migrating zooplankton (light blue), mesopelagic fish (middle blue), carnivores (blue), and by the total (dark blue), which is the sum of migrating zooplankton, mesopelagic fish, and carnivores parts. Error bars show the uncertainty range resulting of the differences in the vertical migration depth.

by the active transport by migrating organisms (Table C3). Between 40°S and 40°N, the active flux is 39%–40% of the total flux (Figure 8b). This ratio is much smaller in the Southern Ocean (10%–11%). Globally the active flux is about one quarter of the total flux. In all regions, the impact of mesopelagic fish on the active transport is larger compared to that of migrating zooplankton. When investigating the ratio of the active export relative to passive sinking, this ratio increases to ∼31% globally and to 57% between 40°S and 40°N, while keeping a similar ratio of 11% in the Southern Ocean (Figure C3).

In contrast to the shallow export, the export at the 550 m depth horizon, the layer below the migration depth of Z_e, shows a different pattern. In the low latitudes, we find an increase relative to noDVM of the total export by 8%–10%. Clearly, in simulations that include DVM, the sinking of organic matter through a depth horizon of 550 m benefits from the fact that zooplankton and fish provide an additional transport mechanism to the mesopelagic, thereby enhancing deep export despite the reduced export production. However, in the Southern Ocean, carbon export at 550 m in simulations that apply migratory processes is lower compared to noDVM. The combination of the small relevance of migration, active flux, and the decline in detritus results in an overall decline of the carbon export compared to noDVM. Similar to the depth horizon of 550 m, we find also for the deepest horizon of 1,500 m a relative increase in the carbon export in the low latitudes between 40°S and 40°N and a relative decrease in the Southern Ocean. Overall, the impact of Southern Ocean on the global response is now larger, resulting in a net decrease in the deep carbon export on a global scale.

Comparing the three sensitivity simulations ($DVM_{200}F1$, $DVM_{200}F2$, $DVM_{300}F2$) that include both migrating processes (migration of zooplankton and that of fish) shows an uncertainty range of maximum 4% for the total export, resulting from differences in the applied migration depth. This is relatively low and indicates that a good choice of the migration depth in this case is of less importance. In addition, we find a very similar uncertainty range for NPP of up to 4%. This further indicates that changes in the surface nutrients driven by vertical migration have a stronger impact on the total export compared to the choice of the vertical migration pattern.

3.3.3. Oxygen

The globally averaged oxygen concentration in UVic is slightly higher compared to the values obtained from observations (Bianchi et al., 2012), yet within the uncertainty range in the CMIP5 models (Bopp et al., 2013). Shallow remineralization in noDVM causes a large value of global average oxygen (Table 4), which is at the higher end of the CMIP5 models. The migratory processes lead to a further increase of the global oxygen inventory of 1%–2.5%, most likely because of the reduced total export production. This increase is slightly enhanced in the Southern Ocean (1.9%–2.7%) and lower in the mid latitudes between 40°S and 40°N (0.7%–2.3%). As noted above, in the Southern Ocean, the model's response to the migratory processes is a reduction in carbon export, thus these water masses face less remineralization. Consequently, the water masses in the Southern Ocean contain more oxygen and also ventilate the lower latitudes with these oxygen rich water masses (Duteil et al., 2021). In contrast, low latitudes experience more deep export when considering vertical migration, which

Table 4
Globally Averaged Oxygen Concentration [mmol/m^3] and Oxygen Inventory [Pmol O_2] for All Simulations

O_2	WOA	UVic	noDVM	noDVM-F1	$DVM_{200}F1$	$DVM_{200}F2$	$DVM_{300}F2$
Average	175	184	198	202	203	200	201
Inventory:							
Global	222	250	269	274	276	272	272
40°S–40°N	144	161	174	177	178	175	176
Southern Ocean	61.0	70.8	75.9	77.7	77.9	77.3	77.3

Note. WOA shows the values derived from the World Ocean Atlas (Garcia et al., 2018).

results in a larger deep respiratory demand. Overall, the response of the global oxygen inventory to migratory processes is small. Similar results can be found by a point-by-point comparison as shown in the Taylor diagram in Figure 9a.

However, unlike the response in the global oxygen inventory, we find that migratory processes impact the low oxygenated areas in the tropical Pacific. Figure 9b shows the area for oxygen values <50 mmol/m^{-3} for the southern (gray shaded, left side of the figure) and the northern equatorial Pacific (right side of the figure). UVic underestimates the area of the southern oxygen minimum zone (OMZ), whereas it overestimates the area of the northern OMZ compared to observational data (Garcia et al., 2018). Comparing the areas of the OMZs between UVic (pink dashed lines in Figure 9b) and noDVM (green lines) over depth, we find a uniform decrease of ∼22% in both hemispheres in the core of the OMZs (300 m in the southern and 850 m in the northern hemisphere) for noDVM, likely because a large part of remineralization in noDVM occurs in shallow waters.

The introduction of migratory processes leads to an opposing response of northern and southern hemispheric OMZs. Compared to noDVM, simulated migration (blue and red lines in Figure 9) leads to a decrease of the area by 5%–17% in the core of the southern Pacific OMZ (300 m), whereas these processes lead to an increase by 10%–17% in the core of northern Pacific OMZ (850 m). This diverging response is a result of the active downward transport of detritus by zooplankton. For the shallower OMZ in the southern Pacific, the active transport by migration reduces the amount of detritus that sinks into and remineralizes within in the core layer, resulting in less oxygen consumption and hence a decrease in the area of the OMZ compared to noDVM. In contrast, in the northern tropical Pacific, the redistribution of detritus by migration takes place in the layers above the core of the OMZ. As migratory processes transport detritus to the deeper layers with lower temperatures compared to surface layers, detritus escapes the fast remineralization at the surface. This, in turn, leads to increased remineralization in these layers compared to noDVM, resulting in an increase in the area of this OMZ.

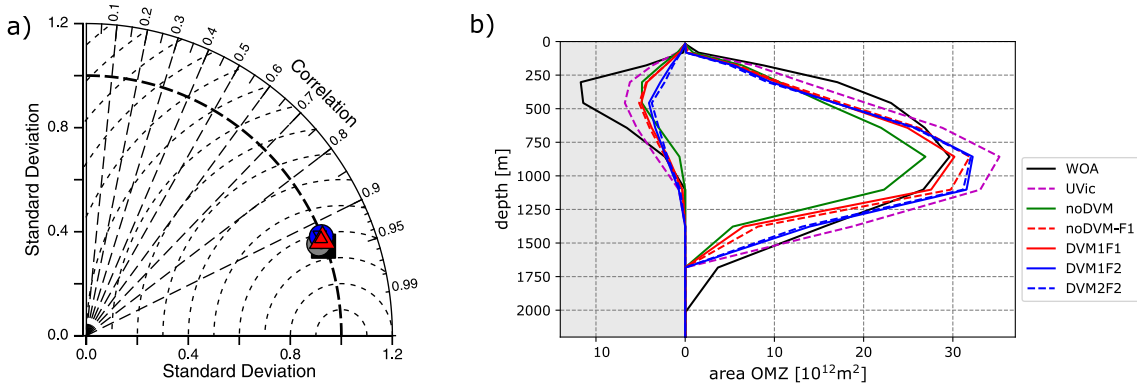

Figure 9. (a) Taylor plot for global oxygen concentrations compared against World Ocean Atlas (Garcia et al., 2018), mapped onto UVic's spatial grid. Different symbols denote model runs: black circle—UVic; gray circle—noDVM; blue circle—DVM-F1; blue inverted triangle—DVM200F1; red triangle—DVM200F2; small red triangle—DVM300F2. (b) Area of the OMZ for oxygen values O_2 < 50 mmol/m^{-3}; gray shaded part shows the area of the OMZ for the southern tropical Pacific and white shaded part the area for the northern tropical Pacific (analogous to Cabré et al. (2015)). The black line shows observational values from the World Ocean Atlas (Garcia et al., 2018).

In general, mesopelagic fish and their transport of organic matter to the mesopelagic appear to be of greater importance for the OMZ area in the Northern Hemisphere than DVM by zooplankton. This can be inferred from a comparison of OMZ areas simulated by noDVM-F1 and noDVM. Introducing vertical fish movement in the former expands the northern OMZ area by 10% (compare dashed red line with green line). Extending the fish profile to deeper layers, as in the shift from $DVM_{200}F1$ to $DVM_{200}F2$ (red and blue lines, respectively), further extends the northern OMZ area. In contrast, introducing vertical migration of zooplankton has a minor effect on the northern OMZ area, as evident from the comparison of $DVM_{200}F1$ (red line) and noDVM-F1 (dashed red line); additionally, the depth of zooplankton migration ($DVM_{200}F2$ vs. $DVM_{300}F2$) seems to play only a small role. Thus, we can conclude that the impact of the vertical distribution of the mesopelagic fish on the extent of the OMZ is larger in our case compared to the impact of differences in the migration depth of the migrating zooplankton.

4. Discussion

Our model results indicate that the dynamics of the mesopelagic ecosystem have a considerable impact on the biogeochemistry. The main drivers are the migrating groups that actively transport carbon and nutrients to greater depth, thereby contributing to the total carbon export. However, potential uncertainties as well as the large regional differences are discussed in the following.

4.1. Zooplankton Representation

Although the global zooplankton biomass representation in our model is at the upper end of the observational range, we find a completely different picture in the Southern Ocean. Recent observations between 50°S and 70°S (Yang et al., 2022) show a total zooplankton biomass of 98.7 Mt C, consisting of 67 Mt C mesozooplankton (68%), 30 Mt C krill (30%) and 1.7 Mt C salps (2%). In UVic-mfish, we find a total zooplankton biomass ranging between 41.9 and 42 Mt C (in all simulations that include at least one migratory process), which is an underestimation of more than 50%. While the zooplankton biomass in the standard UVic configuration is larger (73.6 Mt C) and close to the observed value of the mesozooplankton, the total value is still underestimated.

In our model, we only account for mesozooplankton, which partly performs vertical migration and exhibits similar behavior compared to krill. However, considering migrating zooplankton such as krill in the Southern Ocean still results in an underrepresentation of that group, which likely results to too low deep carbon export as well as too large oxygen uptake. The relative biomass of salps compared to that of mesozooplankton and krill is very low and thus potentially negligible. However, their blooms can result in a high local export of organic matter (Steinberg et al., 2023). Due to their deep migration depth of up to 750 m and their large, fast sinking fecal pellets (e.g., Phillips et al., 2009), salps can affect the export ratio and mesopelagic transfer efficiency of NPP, ultimately carbon sequestration in an extensive way (Buesseler et al., 2020). The challenge in observing their contribution to exports lies in the fact that salps are highly patchy in space and time, as they rapidly respond to favorable environmental conditions (Deibel & Paffenhöfer, 2009).

While we focus in this study on diel vertical migration, we neglect the impact of seasonal vertical migration that occurs mainly in the high latitudes. Seasonal vertical migration, in general, describes the occurrence of organisms at different depth depending on the season. The so called the lipid pump refers to the vertical transport and metabolism of carbon rich lipids by overwintering zooplankton. This pump is highly efficient due to the almost complete decoupling of the nutrient and carbon cycles, and the direct transport of carbon to the mesopelagic. Jónasdóttir et al. (2015) shows that seasonal vertical migration accounts for almost 50% of the deep carbon export by biological processes in the North Atlantic.

So far, deep detritivorous zooplankton are neglected in this model. Regarding the modeled mesopelagic fish biomass, their contribution is of minor importance as they contribute only to 6% of their diet (Anderson et al., 2019). However, when considering feedback processes of the mesopelagic ecosystem on the biogeochemical cycles, these organisms might play a larger role. A key function of detritivorous zooplankton is the fragmentation of detritus (Lampitt et al., 1990; Paffenhöfer & Strickland, 1970), which is an important process for the remineralization of fast sinking particles at depth. Observations from ARGO float data indicate that the

transformation of large, fast-sinking particles into small, slow-sinking fragments is responsible for a decrease of 49% (±22%) in the deep particle flux (Briggs et al., 2020). Giering et al. (2014) showed in a simple, steady-state flow-analysis model that detritivorous zooplankton fragment and ingest about 50% of the fast-sinking particles and release more than 30% of that fraction as slow sinking particles. Additionally, a fraction is directly remineralized by excretion, leading to a shallower remineralization depth. In our model, we only consider slow sinking detritus. When including detritivorous zooplankton in a model, it is important to include fast sinking detritus as well. While fast sinking fecal pellets increase the carbon export, the fragmentation into smaller, slow sinking fecal pellets counteracts this increase in the mesopelagic. Therefore, the resulting net effect on carbon export when including both detritivorous zooplankton and fast sinking detritus might be rather small. Another aspect to consider when neglecting detritivorous zooplankton is that fish feed on them. In our model setup, fish immediately egest detritus, so the resulting effect of detritivorous zooplankton would, in this case, be more or less zero. However, if fish egest at a shallower depth compared to their feeding depth, it results in an uplift of nutrients, whereas an egestion at greater depth compared to their feeding depth results in a downward shift of nutrients.

4.2. Mesopelagic Fish and Their Impact

Global estimates for the mesopelagic fish biomass are not only rare but also cover a large range, from the very early estimate of 1 Gt by Gjøsæter and Kawaguchi (1980) to a more recent one of 10 Gt by Irigoien et al. (2014). Uncertainties in both estimates are large, and currently it is not clear which value is the more likely one. The recent flux estimates derived from primary production by A2019 result in a value for the mesopelagic fish biomass of 2.4 Gt wet weight between 40°S and 40°N with an uncertainty envelope of −30%–50%. Migrating and epipelagic zooplankton are explicitly resolved in UVic-mfish, and thus the ratio of the growth terms is not fixed in space and time. The resulting fish biomass is 2.3–2.6 Gt wet weight between 40°S and 40°N.

One of the most important, yet uncertain, parameters for fish stock assessment is the natural fish mortality. Assessing a value for the mortality directly from observations is rather difficult, as mortality is a function of age, sex, predator numbers, food availability, diseases and other environmental effects, and would require monitoring the whole life span of an age group of fish. Therefore, deriving mortality indirectly from life-history parameters such as longevity has become common practice (Hamel & Cope, 2022; Hoenig, 1983; Kenchington, 2014; Then et al., 2014). The approach by A2019, deriving the mortality from the inverse of longevity, appears to be similar but neither accounts for the production of reproductive material nor the fact that not all fish reach the longevity age, thus underestimating the impact of life cycle interactions as shown in a regional study by Hill Cruz et al. (2023). Applying the rule-of-thumb approach (e.g., Hoenig, 1983, estimating the mortality by $3 \cdot t_{max}^{-1}$), or the approach by Then et al. (2014) (estimating the mortality by $4.899 \cdot t_{max}^{-0.916}$) results in a significantly larger mortality rates. Mesopelagic fish have a lifespan of 1–5 years (Caiger et al., 2021; Catul et al., 2011) derived from global observations and of 2–7 years in the Southern Ocean (Caiger et al., 2021; Saunders et al., 2019). Assuming a longevity that ranges between 1 and 6 years, we get an uncertainty range for the globally integrated mesopelagic fish that ranges between 0.66 and 3.96 Gt wet weight applying the rule-of-thumb approach, and between 0.4 and 2.1 Gt wet weight applying the approach by Then et al. (2014).

In the Southern Ocean, we find the largest fish biomass along the southern regions of the Antarctic Circumpolar Current, which is in line with Dornan et al. (2022). However, their study shows additional biomass peaks dominated by non-gas bearing species along the seasonal ice-edge that are not present in our model. One simple reason for the misrepresentation by our model might be the lack of food for mesopelagic fish in that area. Myctophids are not only the most abundant mesopelagic fishes in the global ocean (Gjøsæter & Kawaguchi, 1980; Irigoien et al., 2014), but in the Southern Ocean, they are the major consumers of krill as indicated by observations (Hill et al., 2007; Kock et al., 2012; Saunders et al., 2019). In UVic-mfish, we only account for mesozooplankton and do not include the explicit representation of krill. With this, we miss an important part of the food chain for mesopelagic fish and underestimate their biomass in this region.

4.3. Consequences for the Carbon Export

In addition to sinking particles as one component of the biological carbon pump, active transport by migrating organisms plays an important role. On a global scale, the active export at the base of the euphotic zone amounts to 10%–30% (Archibald et al., 2019; Aumont et al., 2018; Davison et al., 2015). In our study, we find an overall

contribution of migrating organisms of ∼30% to the export of carbon by passive sinking at the 125 m depth horizon, and similar contributions are found by Aumont et al. (2019) and Gorgues et al. (2019) (the latter only when considering 30% of the total mesozooplankton to migrate). In the modeling approach by Pinti et al. (2023) (a 1D model coupled one-way to a global circulation model), the contributions by metazoans and fish (including mesopelagic fish, forage fish, large pelagic fish and jellyfish) to the global export by passive sinking is ∼20% and slightly smaller compared to the other modeling studies, but well within the large uncertainty range. Saba et al. (2021) shows in a comprehensive overview of observational studies that the active export of midwater fish amounts to 16% of the total flux by passive sinking with a large uncertainty range of ±13%. Assessing only the contribution of mesopelagic fish, we find in our study a fraction of 13%, whereas it amounts to only 3% in Aumont et al. (2019). A2019 also gives estimates of the global carbon flux with a carbon export of 0.48 Gt C/year for invertebrate carnivores and of 0.69 Gt C/year for mesopelagic fish. Especially the latter value is much larger compared to the estimate of 0.19 Gt C/year achieved by Aumont et al. (2019). Our values of 0.49 Gt C/year for invertebrate carnivores and of 0.71 Gt C/year for mesopelagic fish are similar to the values given by A2019. Nowicki et al. (2022) investigated the impact of zooplankton vertical migration on the carbon export and a contribution of 10% to the total export of carbon. In their study, they consider that only larger zooplankton can undertake vertical migration. We find a relative contribution of migrating zooplankton to the total carbon export of 7.4%, which is slightly smaller compared to the findings of Nowicki et al. (2022).

A consequence of the active transport of carbon by vertical migration is a decline in the related total carbon export production by sinking particles. Gorgues et al. (2019) investigated the impact of vertically migrating mesozooplankton on carbon export in a model of the North Atlantic and found a decline in export at the 150 m depth horizon of 18% and 30%, depending on whether 30% or 60% of the total mesozooplankton were considered to migrate vertically. Our results show a smaller decline in the shallow export of 4%–11% when accounting only the North Atlantic, although the ratio of migrating to total zooplankton in our model is similar, at 37%. Remineralization of organic matter is temperature dependent and larger in warmer waters compared to cooler ones (Bendtsen et al., 2015; Marsay et al., 2015; Turner, 2015). Consequently, the organic matter transported by migration to greater depth faces less remineralization, thus leading to an increase in the efficiency of deep carbon export. We find an increase of the deep carbon export (at the 1,500 m depth horizon) by 6%–12% in the low latitudes. Our findings are similar to Gorgues et al. (2019) who found a decrease of 5%–8% (at the 1,000 m depth horizon, assuming migration of 30% or 60% of the total mesozooplankton) in the North Atlantic.

Our model results show an opposing response of the deep carbon export to the migratory processes between the low latitudes and the Southern Ocean. This might possibly be linked to the deficient ecosystem representation on the Southern Ocean. By underestimating the biomass of migrating zooplankton to a large extent, we also underestimate the biomass of mesopelagic fish. The explicit representation of krill might be of particular importance. Krill are vertically migrating with a period of about 12–15hr (Piccolin et al., 1986) and produce large pecal pellets (Belcher et al., 2017). With this, they contribute on average by about 35% to the total export flux of carbon in the marginal ice zone (Belcher et al., 2019). So, our rather rudimentary representation of the Southern Ocean ecosystem very likely neglects processes that are important in shaping the ecosystem's response to migratory mesopelagic processes and will impact the carbon export.

There are many sources of uncertainty related to mesopelagic vertebrates (and invertebrates) that impact the deep carbon sequestration and that are, so far, not considered in current studies. Among them is the representation of the metabolism of mesopelagic organisms that affects the form (dissolved or particulate) in which carbon is redistributed in the water column. A2019 only estimates the contribution of mesopelagic organisms to the export in terms of carbon but does not differentiate between respiration, egestion, or excretion. Gathering information about metabolic rates from mesopelagic fish is rather difficult as it is not easy to obtain healthy (and living) organisms from traditional net sampling. Currently, there is only one method to measure respiration of fish from the mesopelagic (respiratory electron transport system (ETS) measurements, Belcher et al., 2020), thus the lack of data (Ikeda, 2016) is not surprising and is also the case for excretion or egestion rates. The latter is of particular importance as fish fecal pellets sink much faster (orders of magnitude) compared to small particles (Saba & Steinberg, 2012) and are likely to play an important role for the deep carbon sequestration (Bianchi et al., 2021). In line with that, Karakuş et al. (2021) showed that the relatively fast sinking fecal pellets of polar macrozooplankton lead to an increase in the carbon transfer below the mesopelagic zone. Additionally, Saba

et al. (2021) pointed out that not only the sinking speed of fish fecal pellets but also their carbon content (so far this has been investigated only by Bray et al. (1981), Staresinic et al. (1983), and Saba and Steinberg (2012)) will affect the export of carbon. Due to the lack of knowledge, we do not include the metabolism of mesopelagic fish in our approach but would like to stress that more information is needed to further improve current modeling approaches.

4.4. Contribution to Biogeochemical Feedbacks

The migratory processes transport organic matter and with this nutrients to greater depths. This vertical redistribution has the effect of reducing the amount of remineralized nutrients in the surface waters, resulting in a reduction of NPP. This effect is most pronounced in the low latitudes (40°S–40°N), leading to a reduction of NPP of 14%–29%. Our findings are in line with those of Gorgues et al. (2019), who investigated the impact of vertically migrating mesozooplankton in the North Atlantic and found a decrease in NPP of 12% and 20%, depending on whether 30% or 60% of the total mesozooplankton were considered to migrate vertically.

Oxygen minimum zones are caused by the continuous oxygen consumption due to remineralization, combined with weak ventilation (Brandt et al., 2015; Kalvelage et al., 2015). While there are numerous observational studies in the tropical Pacific investigating processes leading to OMZ (Czeschel et al., 2012; Garçon et al., 2019; Schmidtko et al., 2017), a complete understanding of the underlying mechanisms remains elusive (Oschlies et al., 2018). Our findings indicate that vertical migration induces an asymmetric response when comparing the southern and the northern hemispheric OMZs in the tropical Pacific. This is in line with Bianchi, Galbraith, et al. (2013), who also find an asymmetric response in the tropical Pacific OMZs when simulating the impact of DVM respiration on dissolved oxygen.

All simulations presented in this paper were run for 10,000 years. In contrast, Aumont et al. (2019) conducted spin-up of in total 1,300 years, which is sufficient for assessing the shallow carbon export. However, for a full adjustment of the carbon cycle, particularly accounting for changes in the deep carbon sequestration, a spin-up of at least 5,000 years is necessary. Moreover, OMZs show strong trends after 3,000 years of simulation time and require extended adjustment periods (Kriest et al., 2023). Our modeling approach allows for a full model spin-up within a reasonable timeframe in a full Earth system model. This enables the model to fully adjust to DVM and mesopelagic processes, including their interaction with the large scale circulation. Furthermore, this also enables us to perform several sensitivity simulations, which are crucial given the substantial uncertainties in model parameters and assumptions related to, for example, migration patterns.

5. Conclusion

In this study, we present a computationally feasible approach that fully incorporates the core processes of the mesopelagic ecosystem in a two-way coupled fashion in an Earth system model. Our model results indicate that the dynamics of the mesopelagic ecosystem have a considerable impact on the biogeochemistry. The main drivers are the migrating groups that actively transport carbon and nutrients to greater depths. The vertical redistribution of nutrients has a large impact on the net primary production (and also model parameters to "correctly" represent NPP) and also affects the extent of low oxygenated areas. Migratory processes also have a considerable impact on the carbon cycle. Previous studies have mainly considered the impact of the shallow carbon export. However, the redistribution of organic matter in the water column also impacts the deep carbon sequestration, which is important for longer timescales. Uncertainties in the deep carbon export with a source in the mesopelagic ecosystem largely stem from limited knowledge about the metabolism of mesopelagic fish and other mesopelagic organisms. To improve the representation of these carbon cycle dynamics, it is necessary to increase our knowledge about the metabolism of mesopelagic fish. This is especially true for the Southern Ocean, which has an important impact on the global carbon sequestration. However, our results indicate deficiencies in the current representation of the ecosystem dynamics in this region and that the representation of krill should be taken into account in future studies. In our study, we assume a mortality rate of mesopelagic fish which is at the lower end of potential estimates. The mesopelagic fish biomass estimated in this study can be considered a potential upper boundary due to the large uncertainties and differences in the approaches to derive a mortality rate from longevity. Our results suggest that the very large value given in Irigoien et al. (2014) may

overestimate the mesopelagic fish biomass, while lower estimates like those by Gjøsæter and Kawaguchi (1980) might be more likely.

Appendix A: Details for the Model by Anderson et al. (2019)

The model introduced by Anderson et al. (2019) follows a steady-state flux model approach. Apart from estimating mesopelagic fish, no standing stocks are calculated. The model is forced by net primary production (NPP) as source for zooplankton growth and differentiates between three zooplankton classes: (a) the epipelagic zooplankton (Z_e), (b) vertically migrating zooplankton (Z_m) and (c) detritivorous zooplankton (Z_{Det}) that are permanently resident in the mesopelagic zone. Grazing of epipelagic and migrating zooplankton is a linear function of NPP, so that the growth of these two zooplankton groups, G_{Ze} and G_{Zm} respectively, is given as

$$G_{Ze} = f_{PP,Z}\left(1 - f_{Zm}\right) K_Z NPP, \tag{A1}$$

$$G_{Zm} = f_{PP,Z}\left(1 - f_{Zm}\right) K_Z NPP, \tag{A2}$$

where $f_{PP,Z}$ denotes the fraction of NPP that is consumed by copepods, f_{Zm} the fraction of total copepod grazing in the epipelagic zone by migrating zooplankton, and K_Z the gross growth efficiency of copepods. Grazing of detritivorous zooplankton is determined by export production their related growth is given by

$$G_{Zd} = t_{D,Z}\, f_{PP,D} NPP, \tag{A3}$$

where $f_{PP,D}$ denotes the fraction of NPP that is exported as detritus, and $t_{D,Z}$ the transfer efficiency from detritus to copepods. According to Anderson et al. (2019), the total amount of available food from copepods that is available for mesopelagic fish and invertebrate carnivores is then

$$R_Z = G_{Zd} + f_{M,VF} G_{Zm} + f_{R,VF} G_{Ze}, \tag{A4}$$

where $f_{M,VF}$ denotes the grazing of migrating predators (mesopelagic fish and invertebrate carnivores) on migrating zooplankton, and $f_{R,VF}$ their grazing on epipelagic zooplankton. The fraction $f_{Z,F}$ of R_Z is consumed by mesopelagic fish, and the remainder, $1 - f_{Z,F}$, by invertebrate carnivores. Thus, the growth of invertebrate carnivores, G_V is given by

$$G_V = \left(1 - f_{Z,F}\right) K_V R_Z, \tag{A5}$$

with K_V as gross growth efficiency of the invertebrate carnivores. Mesopelagic fish feed partly directly on all three zooplankton groups and partly on invertebrate carnivores. Therefore, their growth is given by

$$G_F = f_{Z,F} K_F R_Z, \tag{A6}$$

where K_F denotes the gross growth efficiency of mesopelagic fish. Assuming a steady state, mesopelagic fish biomass can then be derived by dividing their growth by the mortality rate, as given by Equation 10. An overview of all model parameters as in Anderson et al. (2019) is given in Table A1.

Table A1
Overview of All Parameters for the Modeling Approach Introduced by Anderson et al. (2019) (Copy of Their Default Parameters Given in Their Table 2)

Parameter	Definition	Value	Unit
NPP	Net primary production	43	Gt C year−1
$f_{PP,D}$	Fraction of NPP export as detritus	0.11	Dimensionless
$f_{PP,Z}$	Fraction of NPP to copepods	0.32	Dimensionless
f_{ZM}	Fraction of $f_{PP,Z}$ due to migrators	0.18	Dimensionless
K_Z	Gross growth efficiency of copepods	0.26	Dimensionless
K_V	Gross growth efficiency of carnivores	0.22	Dimensionless
K_F	Gross growth efficiency of mesopelagic fish	0.2	Dimensionless
$t_{D,Z}$	Transfer efficiency from detritus to copepods	0.0145	Dimensionless
$f_{M,VF}$	Fraction of Z_m to carnivores and fish	0.88	Dimensionless
$f_{R,VF}$	Fraction of Z_e to carnivores and fish	0.18	Dimensionless
$f_{Z,F}$	Fraction of Z_m grazed by fish	0.5	Dimensionless
$f_{V,F}$	Fraction of invertebrate carnivores grazed by fish	0.8	Dimensionless
m_F	Mesopelagic fish mortality	0.67	$year^{-1}$

Appendix B: Zooplankton Grazing Formulation

Z_{sum} denotes the sum of both zooplankton groups Z_e and Z_m. The total grazing of both zooplankton groups is then given by

$$graz_{Zsum} = g_{max}\, Z_{sum} (0.5 \cdot I_p\, P + I_D\, D + I_{Det}\, Det + I_{Ze}\, Z_e) \tag{B1}$$

We further assume that Z_m is a fraction or multiple x of Z_e ($Z_m = x \cdot Z_e$) and migrating zooplankton is only grazing the fraction τ_Z of the day in the epipelagic. Further only epipelagic zooplankton feed on P, D, Z_e and Det; thus Equation B1 can be written as:

$$graz_{Zsum} = g_{max}\, (1 + \tau_Z\, x) \cdot 0.5\, Z_e\, I_p\, P + g_{max} Z_e (I_D\, D + I_{Det}\, Det + I_{Ze}\, Z_e) \tag{B2}$$

Assuming that 2/3 of the total zooplankton is epipelagic and 1/3 is migration zooplankton, results in x = 2 as

$$\begin{aligned} Z_m &= x \cdot Z_e \\ \frac{2}{3} Z_{sum} &= x \cdot \frac{1}{3} Z_{sum} \\ x &= 2 \end{aligned}$$

Further assuming that τ_Z averages to 0.5, the total grazing pressure on phytoplankton would then equal the original grazing pressure on phytoplankton in UVic. We note that this is a rather pragmatic approach that overlooks many biological and ecological features, including competition for food among the two groups. Addressing this issue, particularly competition among two groups of herbivores, is an important topic and should be addressed in future work.

Appendix C: Zooplankton

Here, you find an overview of the spatial zooplankton distribution (Figure C1) as well as a summary of the integrated zooplankton biomass for each simulation (Table C1) and an overview of all state values (Table C2). In addition you find a detailed comparison of the observed and simulated particle flux (Figure C2), the active export for $\overline{\text{DVM}}$ relative to passive sinking at 125 m (Figure C3), an overview of the active carbon transport at the 125 m depth horizon (Table C3) and the change of the globally integrated detritus concentration related to vertical migration (Figure C4).

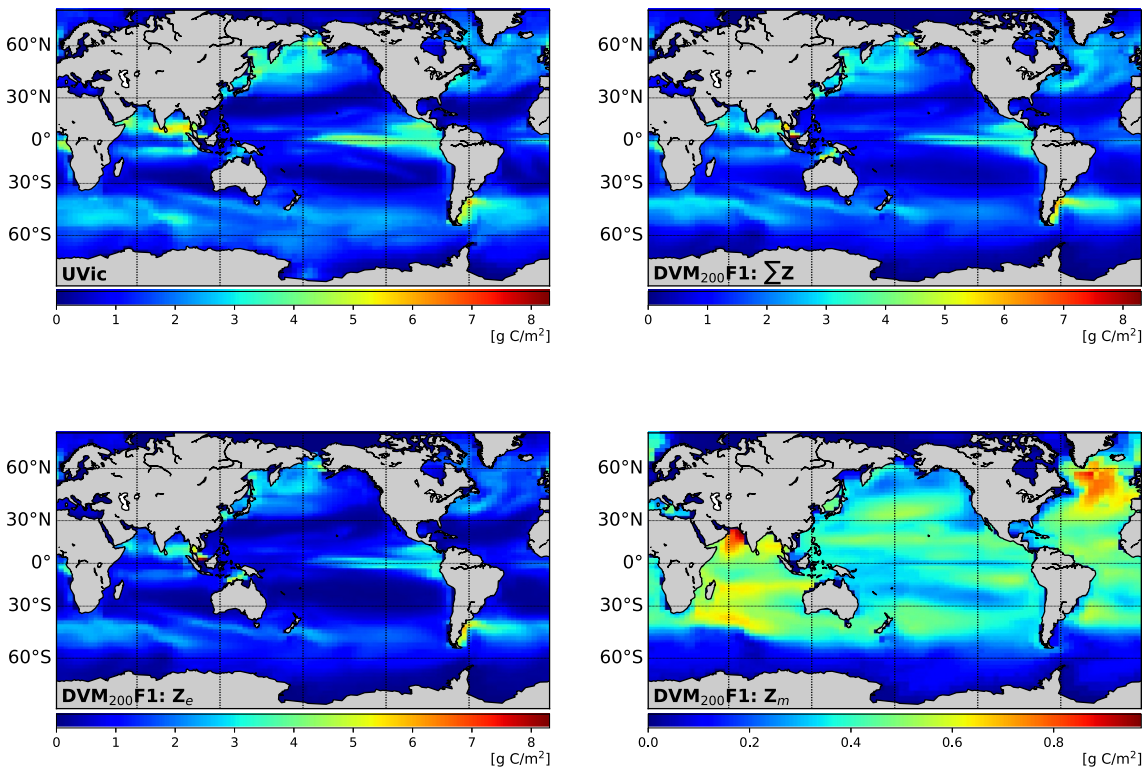

Figure C1. Vertically integrated, annual mean zooplankton biomass for UVic (top left) and for $DVM_{200}F1$ (top right: sum of Z_e and Z_m; bottom left: Z_e; bottom right: Z_m). Note the different color scale for Z_m (lower right panel).

Table C1
Overview of Annual Mean Zooplankton Biomass for Total Zooplankton Z_t, the Two Zooplankton Groups Z_e and Z_m and Mesopelagic Fish

	UVic	noDVM	noDVM-F1	$DVM_{200}F1$	$DVM_{200}F2$	$DVM_{300}F2$
Z_t (Gt C):						
Global	0.53	0.57	0.53	0.52	0.50	0.50
40°S–40°N	0.31	0.37	0.34	0.33	0.32	0.31
Southern Ocean	0.15	0.13	0.12	0.12	0.12	0.12
Z_e (Gt C):						
Global	0.53	0.43	0.40	0.39	0.38	0.37
40°S–40°N	0.31	0.27	0.24	0.23	0.22	0.21
Southern Ocean	0.15	0.11	0.11	0.11	0.11	0.11
Z_m (Gt C):						
Global	–	0.14	0.13	0.13	0.13	0.13
40°S–40°N	–	0.11	0.10	0.10	0.10	0.10
Southern Ocean	–	0.02	0.02	0.02	0.02	0.02
Mesop. fish [Gt wet weight]:						
Global	–	4.18	3.60	3.38	3.17	3.05
40°S–40°N	–	3.40	2.83	2.62	2.41	2.29
Southern Ocean	–	0.52	0.51	0.51	0.50	0.51

Note. Zooplankton biomass has been converted to carbon using a C:N ratio of 6.625 mol C:mol N.

Table C2
Overview of All Steady State Values in [Gt C y^{-1}]

(Gt C y^{-1})	UVic	noDVM	noDVM-F1	$DVM_{200}F1$	$DVM_{200}F2$	$DVM_{300}F2$
NPP:						
Global	49.40	58.37	52.83	50.46	47.84	46.15
40°S–40°N	36.01	43.30	37.41	35.08	32.60	30.82
Southern Ocean	8.66	10.11	10.26	10.24	10.20	10.26
Export (125 m):						
Global	6.79	6.83	6.73	6.72	6.58	6.45
40°S–40°N	3.76	3.65	3.60	3.58	3.44	3.30
Southern Ocean	2.04	2.12	2.07	2.07	2.08	2.09
Export (550 m):						
Global	2.81	2.83	2.87	2.84	2.89	2.89
40°S–40°N	1.36	1.32	1.45	1.43	1.45	1.44
Southern Ocean	1.02	1.03	0.96	0.96	0.98	0.98
Export (1,500 m):						
Global	0.75	0.74	0.69	0.68	0.73	0.72
40°S–40°N	0.34	0.32	0.35	0.34	0.36	0.36
Southern Ocean	0.32	0.32	0.26	0.26	0.27	0.27

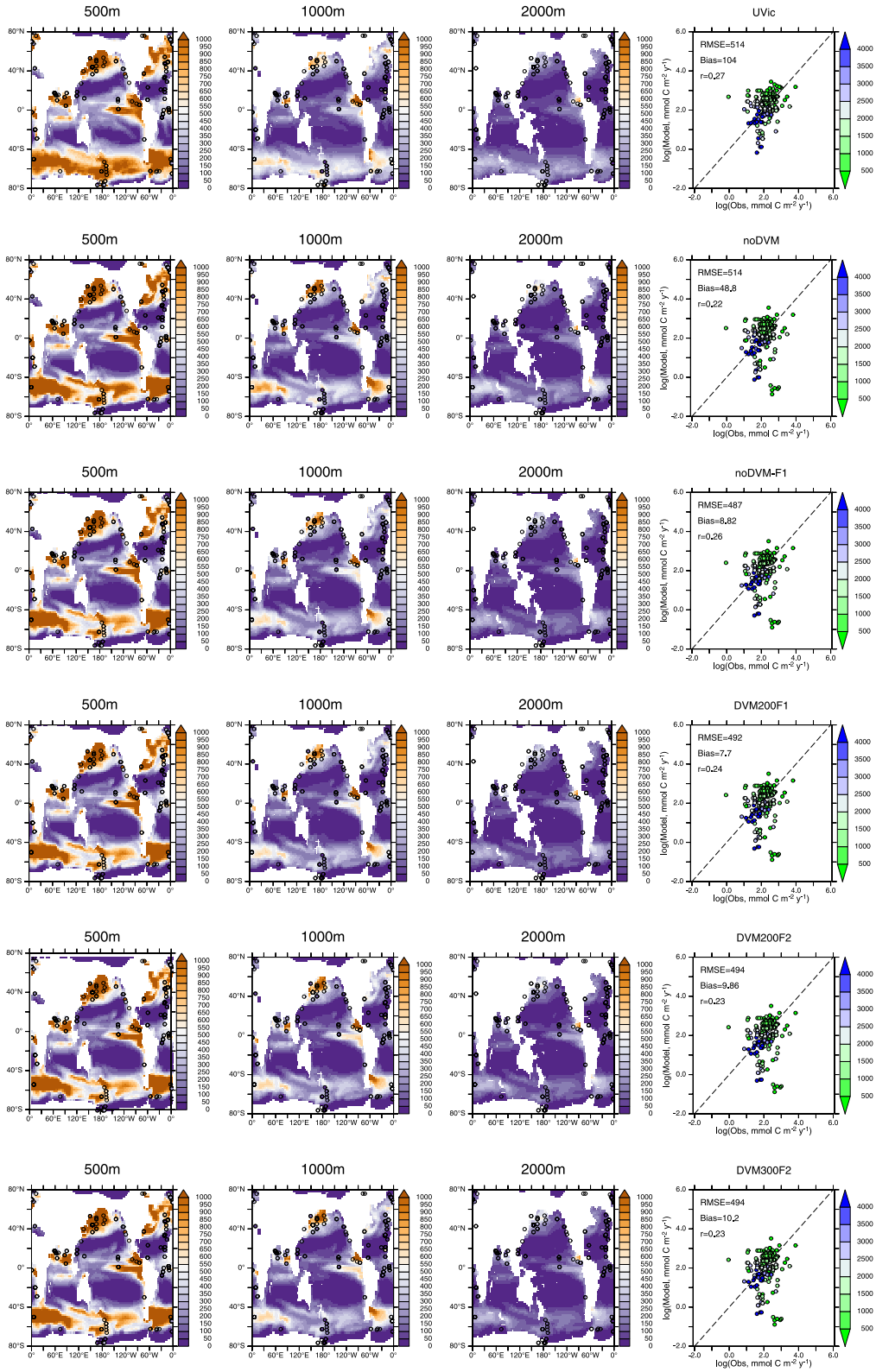

Figure C2. Simulated and observed (colored circles) particle flux. The three panels on the left show particle flux (mmol C m^{-2} y^{-1}) at three different depth levels ±10%. The right panel shows log (simulated flux) versus log (observed flux), both in mmol C m^{-2} y^{-1}. Color code in the right panel indicates the trap depth. Statistics are based on non-transformed values. Observations are by Mouw et al. (2016). For model comparison we only chose observations from sediment traps which were deployed at least 360 days.

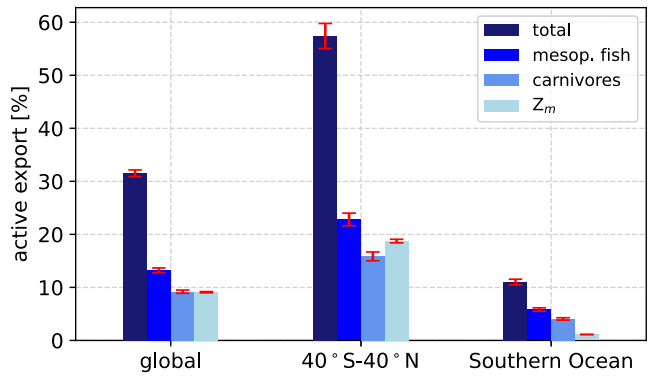

Figure C3. Active export for $\overline{\text{DVM}}$ relative to passive sinking detritus at the 125 m depth horizon by migrating zooplankton (light blue), by mesopelagic fish (middle blue) and by the total, which is the sum of both parts (dark blue). Error bars show the uncertainty range resulting of the differences in the vertical migration depth.

Table C3
Overview of Active Carbon Transport at the 125 m Depth Horizon [Gt C y^{-1}]

Active export (125 m) (Gt C y^{-1})	$DVM_{200}F1$	$DVM_{200}F2$	$DVM_{300}F2$
Global: total	1.70	1.72	1.66
Mesop. fish	0.71	0.74	0.70
Carnivores	0.49	0.51	0.49
Z_m	0.50	0.47	0.46
40°S–40°N: total	1.39	1.38	1.31
Mesop. fish	0.55	0.56	0.53
Carnivores	0.38	0.39	0.37
Z_m	0.46	0.43	0.41
Southern Ocean: total	0.20	0.22	0.22
Mesop. fish	0.11	0.12	0.12
Carnivores	0.07	0.08	0.08
Z_m	0.02	0.02	0.02

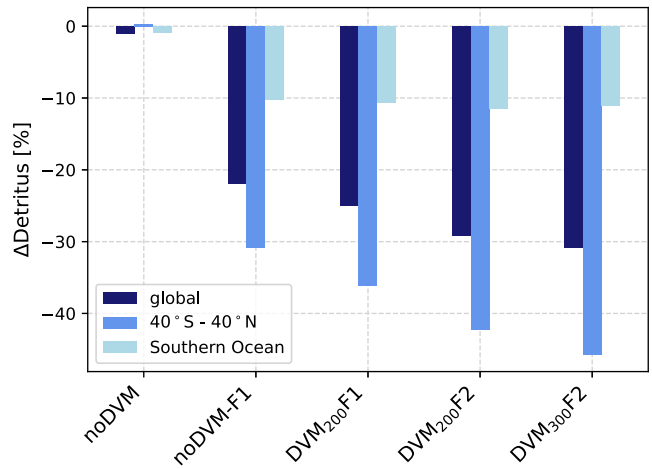

Figure C4. Globally integrated surface (0–130 m) detritus concentration (dark blue), surface detritus integrated between 40°S and 40°N (blue) and integrated across the Southern Ocean south of 40°S (light blue) relative to UVic.

Data Availability Statement

The data and material that support the findings of this study are available through GEOMAR at https://hdl.handle.net/20.500.12085/4b06e625-69da-47d4-a193-dad502b081f6 (Getzlaff & Kriest, 2024). Additional data that are used in this study are available in Garcia et al. (2018) and Mouw et al. (2016).

Acknowledgments
This work is a contribution to BMBF project CO2Meso (FKZ 03F0876A) and to Horizon Europe project OceanICU—Understanding Ocean Carbon (Grant agreement 101083922). We thank Ben Perret for proof reading the manuscript and three anonymous reviewers for their helpful and constructive comments. Open Access funding enabled and organized by Projekt DEAL.

References

Al-Mutairi, H., & Landry, M. R. (2001). Active export of carbon and nitrogen at station aloha by diel migrant zooplankton. *Deep Sea Research Part II: Topical Studies in Oceanography*, *48*(8–9), 2083–2103. https://doi.org/10.1016/s0967-0645(00)00174-0

Alvheim, A. R., Kjellevold, M., Strand, E., Sanden, M., & Wiech, M. (2020). Mesopelagic species and their potential contribution to food and feed security—A case study from Norway. *Foods*, *9*(3), 344. https://doi.org/10.3390/foods9030344

Anderson, T. R., Martin, A. P., Lampitt, R. S., Trueman, C. N., Henson, S. A., & Mayor, D. J. (2019). Quantifying carbon fluxes from primary production to mesopelagic fish using a simple food web model. *ICES Journal of Marine Science*, *76*(3), 690–701. https://doi.org/10.1093/icesjms/fsx234

Archibald, K. M., Siegel, D. A., & Doney, S. C. (2019). Modeling the impact of zooplankton diel vertical migration on the carbon export flux of the biological pump. *Global Biogeochemical Cycles*, *33*(2), 181–199. https://doi.org/10.1029/2018GB005983

Aumont, O., Maury, O., Lefort, S., & Bopp, L. (2018). Evaluating the potential impacts of the diurnal vertical migration by marine organisms on marine biogeochemistry. *Global Biogeochemical Cycles*, *32*(11), 1622–1643. https://doi.org/10.1029/2018GB005886

Aumont, O., Maury, O., Lefort, S., & Bopp, L. (2019). Evaluating the potential impacts of the diurnal vertical migration by marine organisms on marine biogeochemistry. *Global Biogeochemical Cycles*, *32*(11), 1622–1643. https://doi.org/10.1029/2018GB005886

Bar-On, Y., Phillips, R., & Milo, R. (2018). The biomass distribution on Earth. *Proceedings of the National Academy of Sciences of the United States of America*, *115*(25), 6506–6511. https://doi.org/10.1073/pnas.1711842115

Behrenfeld, M. J., & Falkowski, P. G. (1997). Photosynthetic rates derived from satellite-based chlorophyll concentration. *Limnology & Oceanography*, *42*(1), 1–20. https://doi.org/10.4319/lo.1997.42.1.0001

Belcher, A., Cook, K., Bondyale-Juez, D., Stowasser, G., Fielding, S., Saunders, R. A., et al. (2020). Respiration of mesopelagic fish: A comparison of respiratory electron transport system (ETS) measurements and allometrically calculated rates in the Southern Ocean and Benguela Current. *ICES Journal of Marine Science*, *77*(5), 1672–1684. https://doi.org/10.1093/icesjms/fsaa031

Belcher, A., Henson, S. A., Manno, C., Hill, S. L., Atkinson, A., Thorpe, S. E., et al. (2019). Krill faecal pellets drive hidden pulses of particulate organic carbon in the marginal ice zone. *Nature Communications*, *10*(1), 889. https://doi.org/10.1038/s41467-019-08847-1

Belcher, A., Tarling, G. A., Manno, C., Atkinson, A., Ward, P., Skaret, G., et al. (2017). The potential role of Antarctic krill faecal pellets in efficient carbon export at the marginal ice zone of the South Orkney Islands in spring. *Polar Biology*, *40*(10), 2001–2013. https://doi.org/10.1007/s00300-017-2118-z

Bendtsen, J., Hilligsøe, K. M., Hansen, J. L., & Richardson, K. (2015). Analysis of remineralisation, lability, temperature sensitivity and structural composition of organic matter from the upper ocean. *Progress in Oceanography*, *130*, 125–145. https://doi.org/10.1016/j.pocean.2014.10.009

Berntssen, M. H. G., Thoresen, L., Albrektsen, S., Grimaldo, E., Grimsmo, L., Whitaker, R. D., et al. (2021). Processing mixed mesopelagic biomass from the North-East Atlantic into aquafeed resources; implication for food savety. *Foods*, *10*(6), 1265. https://doi.org/10.3390/foods10061265

Bianchi, D., Carozza, D., Galbraith, E., J, G., & T, D. (2021). Estimating global biomass and biogeochemical cycling of marine fish with and without fishing. *Science Advances*, *7*(41). https://doi.org/10.1126/sciadv.abd7554

Bianchi, D., Dunne, J. P., Sarmiento, J. L., & Galbraith, E. D. (2012). Data-based estimates of suboxia, denitrification, and N_2O production in the ocean and their sensitivities to dissolved O_2. *Global Biogeochemical Cycles*, *26*(2). https://doi.org/10.1029/2011GB004209

Bianchi, D., Galbraith, E. D., Carozza, D. A., Milan, K. A. S., & Stock, C. (2013). Intensification of open-ocean oxygen depletion by vertically migrating animals. *Nature Geoscience*, *6*(7), 545–548. https://doi.org/10.1038/ngeo1837

Bianchi, D., Stock, C., Galbraith, E. D., & Sarmiento, J. L. (2013). Diel vertical migration: Ecological controls and impacts on the biological pump in a one-dimensional ocean model. *Global Biogeochemical Cycles*, *27*(2), 478–491. https://doi.org/10.1002/gbc.20031

Bopp, L., Resplandy, L., Orr, J. C., Doney, S. C., Dunne, J. P., Gehlen, M., et al. (2013). Multiple stressors of ocean ecosystems in the 21st century: Projections with CMIP5 models. *Biogeosciences*, *10*(10), 6225–6245. https://doi.org/10.5194/bg-10-6225-2013

Boyd, P. W., Claustre, H., Levy, M., Siegel, D. A., & Weber, T. (2019). Multi-faceted particle pumps drive carbon sequestration in the ocean. *Nature*, *568*(7752), 327–335. https://doi.org/10.1038/s41586-019-1098-2

Brandt, P., Bange, H. W., Banyte, D., Dengler, M., Didwischus, S.-H., Fischer, T., et al. (2015). On the role of circulation and mixing in the ventilation of oxygen minimum zones with a focus on the eastern tropical North Atlantic. *Biogeosciences*, *12*(2), 489–512. https://doi.org/10.5194/bg-12-489-2015

Bray, R. N., Miller, A. C., & Geesey, G. G. (1981). The fish connection: A trophic link between planktonic and rocky reef communities? *Science*, *214*(4517), 204–205. https://doi.org/10.1126/science.214.4517.204

Briggs, N., Dall'Olmo, G., & Claustre, H. (2020). Major role of particle fragmentation in regulating biological sequestration of CO_2 by the oceans. *Science*, *367*(6479), 791–793. https://doi.org/10.1126/science.aay1790

Bronk, D. A., & Steinberg, D. K. (2008). Chapter 8—Nitrogen regeneration. In D. G. Capone, D. A. Bronk, M. R. Mulholland, & E. J. Carpenter (Eds.), *Nitrogen in the marine environment* (2nd ed., pp. 385–467). Academic Press.

Buesseler, K. O., Benitez-Nelson, C. R., Roca-Martí, M., Wyatt, A. M., Resplandy, L., Clevenger, S. J., et al. (2020). High-resolution spatial and temporal measurements of particulate organic carbon flux using thorium-234 in the northeast Pacific Ocean during the export processes in the ocean from remote sensing field campaign. *Elementa: Science of the Anthropocene*, *8*(1). https://doi.org/10.1525/elementa.2020.030

Buesseler, K. O., & Boyd, P. W. (2009). Shedding light on processes that control particle export and flux attenuation in the twilight zone of the open ocean. *Limnology & Oceanography*, *54*(4), 1210–1232. https://doi.org/10.4319/lo.2009.54.4.1210

Buitenhuis, E. T., Vogt, M., Moriarty, R., Bednaršek, N., Doney, S. C., Leblanc, K., et al. (2013). MAREDAT: Towards a world atlas of marine ecosystem data. *Earth System Science Data*, *5*(2), 227–239. https://doi.org/10.5194/essd-5-227-2013

Cabré, A., Marinov, I., Bernardello, R., & Bianchi, D. (2015). Oxygen minimum zones in the tropical Pacific across CMIP5 models: Mean state, differences and climate change trends. *Biogeosciences*, *12*(18), 5429–5454. https://doi.org/10.5194/bg-12-5429-2015

Caiger, P. E., Lefebve, L. S., & Llopiz, J. K. (2021). Growth and reproduction in mesopelagic fishes: A literature synthesis. *ICES Journal of Marine Science*, *78*(3), 765–781. https://doi.org/10.1093/icesjms/fsaa247

Carr, M.-E. (2001). Estimation of potential productivity in eastern boundary currents using remote sensing. *Deep Sea Research Part II: Topical Studies in Oceanography*, *49*(1), 59–80. https://doi.org/10.1016/S0967-0645(01)00094-7

Catul, V., Gauns, M., & Karuppasamy, P. K. (2011). A review on mesopelagic fishes belonging to family Myctophidae. *Reviews in Fish Biology and Fisheries*, *21*(3), 339–354. https://doi.org/10.1007/s11160-010-9176-4

Cisewski, B., & Strass, V. H. (2016). Acoustic insights into the zooplankton dynamics of the eastern Weddell Sea. *Progress in Oceanography*, *144*, 62–92. https://doi.org/10.1016/j.pocean.2016.03.005

Conroy, J. A., Steinberg, D. K., Thibodeau, P. S., & Schofield, O. (2020). Zooplankton diel vertical migration during Antarctic summer. *Deep Sea Research Part I: Oceanographic Research Papers*, *162*, 103324. https://doi.org/10.1016/j.dsr.2020.103324

Czeschel, R., Stramma, L., & Johnson, G. C. (2012). Oxygen decreases and variability in the eastern equatorial Pacific. *Journal of Geophysical Research*, *117*(C11), C11019. https://doi.org/10.1029/2012JC008043

Daewel, U., Hjøllo, S. S., Huret, M., Ji, R., Maar, M., Niiranen, S., et al. (2014). Predation control of zooplankton dynamics: A review of observations and models. *ICES Journal of Marine Science*, *71*(2), 254–271. https://doi.org/10.1093/icesjms/fst125

Davison, P., Checkley, D., Koslow, J., & Barlow, J. (2013). Carbon export mediated by mesopelagic fishes in the northeast Pacific Ocean. *Progress in Oceanography*, *116*, 14–30. https://doi.org/10.1016/j.pocean.2013.05.013

Davison, P., Koslow, J., & Kloser, R. (2015). Acoustic biomass estimation of mesopelagic fish: Backscattering from individuals, populations, and communities. *ICES Journal of Marine Science*, *72*(5), 1413–1424. https://doi.org/10.1093/icesjms/fsv023

Deibel, D., & Paffenhöfer, G.-A. (2009). Predictability of patches of neritic salps and doliolids (Tunicata, Thaliacea). *Journal of Plankton Research*, *31*(12), 1571–1579. https://doi.org/10.1093/plankt/fbp091

Dornan, T., Fielding, S., Saunders, R. A., & J, G. M. (2022). Large mesopelagic fish biomass in the Southern Ocean resolved by acoustic properties. *Proceedings of the Royal Society A: Mathematical, Physical and Engineering Sciences B*, *289*(1967). https://doi.org/10.1098/rspb.2021.1781

Drago, L., Panaïotis, T., Irisson, J.-O., Babin, M., Biard, T., Carlotti, F., et al. (2022). Global distribution of zooplankton biomass estimated by in situ imaging and machine learning. *Frontiers in Marine Science*, *9*. https://doi.org/10.3389/fmars.2022.894372

Duteil, O., Frenger, I., & Getzlaff, J. (2021). The riddle of eastern tropical Pacific Ocean oxygen levels: The role of the supply by intermediate-depth waters. *Science*, *17*(5), 1489–1507. https://doi.org/10.5194/os-17-1489-2021

Fanning, A. F., & Weaver, A. J. (1996). An atmospheric energy-moisture balance model: Climatology, interpentadal climate change, and coupling to an ocean general circulation model. *Journal of Geophysical Research*, *101*(D10), 15111–15128. https://doi.org/10.1029/96JD01017

Galbraith, E., Carozza, D., & Bianchi, D. (2017). A coupled human-Earth model perspective on long-term trends in the global marine fishery. *Nature Communications*, *8*(1), 14884. https://doi.org/10.1038/ncomms14884

Garabato, A. C. N., Polzin, K. L., King, B. A., Heywood, K. J., & Visbeck, M. (2004). Widespread intense turbulent mixing in the Southern Ocean. *Science*, *303*(5655), 210–213. https://doi.org/10.1126/science.1090929

Garcia, H., Weathers, K., Paver, C., Smolyar, I., Boyer, T., Locarnini, R., & Reagan, J. (2018). *World ocean atlas 2018, volume 3: Dissolved oxygen, apparent oxygen utilization, and oxygen saturation*. In A. Mishonov Technical (Ed.) (83). NOAA Atlas NESDIS.

Garçon, V., Karstensen, J., Palacz, A., Telszewski, M., Aparco Lara, T., Breitburg, D., et al. (2019). Multidisciplinary observing in the world ocean's oxygen minimum zone regions: From climate to fish—The voice initiative. *Frontiers in Marine Science*, *6*. https://doi.org/10.3389/fmars.2019.00722

Gent, P. R., & McWilliams, J. C. (1990). Isopycnal mixing in ocean circulation models. *Journal of Physical Oceanography*, *20*(1), 150–155. https://doi.org/10.1175/1520-0485(1990)020⟨0150:IMIOCM⟩2.0.CO;2

Getzlaff, J., & Dietze, H. (2013). Effects of increased isopycnal diffusivity mimicking the unresolved equatorial intermediate current system in an Earth system climate model. *Geophysical Research Letters*, *40*(10), 2166–2170. https://doi.org/10.1002/grl.50419

Getzlaff, J., Dietze, H., & Oschlies, A. (2016). Simulated effects of southern hemispheric wind changes on the Pacific oxygen minimum zone. *Geophysical Research Letters*, *43*(2), 728–734. https://doi.org/10.1002/2015GL066841

Getzlaff, J., & Kriest, I. (2024). Supplementary data to Getzlaff and Kriest: Impacts of vertical migrants on biogeochemistry in an earth system model [Dataset]. *GEOMAR Helmholtz Centre for Ocean Research Kiel [distributor]*. https://hdl.20.500.12085/4b06e625-69da-47d4-a193-dad502b081f6

Getzlaff, J., & Oschlies, A. (2017). Pilot study on potential impacts of fisheries-induced changes in zooplankton mortality on marine biogeochemistry. *Global Biogeochemical Cycles*, *31*(11), 1656–1673. https://doi.org/10.1002/2017GB005721

Giering, S. L. C., Sanders, R., Lampitt, R. S., Anderson, T. R., Tamburini, C., Boutrif, M., et al. (2014). Reconciliation of the carbon budget in the ocean's twilight zone. *Nature*, *507*(7493), 480–483. https://doi.org/10.1038/nature13123

Gjøsæter, J., & Kawaguchi, K. (1980). *A review of the world resources of mesopelagic fish* (Vol. 193, pp. 1–151). Food and Agriculture Organization.

Goes, M., Urban, N. M., Tonkonojenkov, R., Haran, M., Schmittner, A., & Keller, K. (2010). What is the skill of ocean tracers in reducing uncertainties about ocean diapycnal mixing and projections of the Atlantic Meridional Overturning Circulation? *Journal of Geophysical Research*, *115*(C12), C12006. https://doi.org/10.1029/2010JC006407

Gorgues, T., Aumont, O., & Memery, L. (2019). Simulated changes in the particulate carbon export efficiency due to diel vertical migration of zooplankton in the North Atlantic. *Geophysical Research Letters*, *46*(10), 5387–5395. https://doi.org/10.1029/2018GL081748

Guidi, L., Legendre, L., Reygondeau, G., Uitz, J., Stemmann, L., & Henson, S. A. (2015). A new look at ocean carbon remineralization for estimating deepwater sequestration. *Global Biogeochemical Cycles*, *29*(7), 1044–1059. https://doi.org/10.1002/2014GB005063

Hamel, O. S., & Cope, J. M. (2022). Development and considerations for application of a longevity-based prior for the natural mortality rate. *Fisheries Research*, *256*, 106477. https://doi.org/10.1016/j.fishres.2022.106477

Henson, S., Sanders, R., & Madsen, E. (2012). Global patterns in efficiency of particulate organic carbon export and transfer to the deep ocean. *Global Biogeochemical Cycles*, *26*(1). https://doi.org/10.1029/2011GB004099

Hill, S., Reid, K., Thorpe, S., Hinke, J., & Watters, G. (2007). A compilation of parameters for ecosystem dynamics models of the Scotia Sea-Antarctic Peninsula region. *CCAMLR Science*, *14*.

Hill Cruz, M., Kriest, I., & Getzlaff, J. (2023). Diving deeper: Mesopelagic fish biomass estimates comparison using two different models. *Frontiers in Marine Science*, *10*. https://doi.org/10.3389/fmars.2023.1121569

Hill Cruz, M., Kriest, I., José, Y. S., Kiko, R., Hauss, H., & Oschlies, A. (2021). Zooplankton mortality effects on the plankton community of the northern Humboldt Current System: Sensitivity of a regional biogeochemical model. *Biogeosciences*, *18*(9), 2891–2916. https://doi.org/10.5194/bg-18-2891-2021

Hoenig, J. (1983). Empirical use of longevity data to estimate mortality rates. *Fishery Bulletin*, *82*, 898–903.

Ikeda, T. (2016). Routine metabolic rates of pelagic marine fishes and cephalopods as a function of body mass, habitat temperature and habitat depth. *Journal of Experimental Marine Biology and Ecology*, *480*, 74–86. https://doi.org/10.1016/j.jembe.2016.03.012

Ikeda, T., McKinnon, A., & Doherty, P. (2011). Metabolism and chemical composition of small teleost fishes from tropical inshore waters. *Marine Ecology Progress Series*, *435*, 197–207. https://doi.org/10.3354/meps09230

Irigoien, X., Klevjer, T. A., Røstad, A., Martinez, U., Boyra, G., Acuña, J. L., et al. (2014). Large mesopelagic fishes biomass and trophic efficiency in the open ocean. *Nature Communications*, *5*(1), 3271. https://doi.org/10.1038/ncomms4271

Jin, D., Hoagland, P., & Buesseler, K. O. (2020). The value of scientific research on the ocean's biological carbon pump. *Science of the Total Environment*, *749*, 141357. https://doi.org/10.1016/j.scitotenv.2020.141357

Jónasdóttir, S. H., Visser, A. W., Richardson, K., & Heath, M. R. (2015). Seasonal copepod lipid pump promotes carbon sequestration in the deep North Atlantic. *Proceedings of the National Academy of Sciences of the United States of America*, *112*(39), 12122–12126. https://doi.org/10.1073/pnas.1512110112

Kalvelage, T., Lavik, G., Jensen, M. M., Revsbech, N. P., Löscher, C., Schunck, H., et al. (2015). Aerobic microbial respiration in oceanic oxygen minimum zones. *PLoS One*, *10*(7), e0133526. https://doi.org/10.1371/journal.pone.0133526

Karakuş, O., Völker, C., Iversen, M., Hagen, W., Wolf-Gladrow, D., Fach, B., & Hauck, J. (2021). Modeling the impact of macrozooplankton on carbon export production in the Southern Ocean. *Journal of Geophysical Research: Oceans*, *126*(12), e2021JC017315. https://doi.org/10.1029/2021JC017315

Keller, D. P., Oschlies, A., & Eby, M. (2012). A new marine ecosystem model for the University of Victoria Earth System Climate Model. *Geoscientific Model Development*, *5*(5), 1195–1220. https://doi.org/10.5194/gmd-5-1195-2012

Kenchington, T. J. (2014). Natural mortality estimators for information-limited fisheries. *Fish and Fisheries*, *15*(4), 533–562. https://doi.org/10.1111/faf.12027

Klevjer, T. A., Irigoien, X., Røstad, A., Fraile-Nuez, E., Benítez-Barrios, V. M., & Kaartvedt, S. (2016). Large scale patterns in vertical distribution and behaviour of mesopelagic scattering layers. *Scientific Reports*, *6*(1), 19873. https://doi.org/10.1038/srep19873

Kock, K.-H., Barrera-Oro, E., Belchier, M., Collins, M., Duhamel, G., Hanchet, S., et al. (2012). The role of fish as predators of krill (Euphausia superba) and other pelagic resources in the Southern Ocean. *CCAMLR Science*, *19*.

Kriest, I., Getzlaff, J., Landolfi, A., Sauerland, V., Schartau, M., & Oschlies, A. (2023). Exploring the role of different data types and timescales for the quality of marine biogeochemical model calibration. *Biogeosciences Discussions*, *2023*, 1–33. https://doi.org/10.5194/bg-2023-9

Lampitt, R. S., Noji, T., & von Bodungen, B. (1990). What happens to zooplankton faecal pellets? Implications for material flux. *Marine Biology*, *104*(1), 15–23. https://doi.org/10.1007/BF01313152

Lauritano, C., Martínez, K. A., Battaglia, P., Granata, P., de la Cruz, M., Cautain, B., et al. (2020). First evidence of anticancer and antimicrobial activity in Mediterranean mesopelagic species. *Scientific Reports*, *10*(1), 4929. https://doi.org/10.1038/s41598-020-61515-z

Longhurst, A., Bedo, A., Harrison, W., Head, E., & Sameoto, D. (1990). Vertical flux of respiratory carbon by oceanic diel migrant biota. *Deep-Sea Research, Part A: Oceanographic Research Papers*, *37*(4), 685–694. https://doi.org/10.1016/0198-0149(90)90098-G

Lotze, H. K., & Worm, B. (2009). Historical baselines for large marine animals. *Trends in Ecology & Evolution*, *24*(5), 254–262. https://doi.org/10.1016/j.tree.2008.12.004

Madin, L. P., Horgan, E., & Steinberg, D. K. (2001). Zooplankton at the Bermuda Atlantic Time-series Study (BATS) station: Diel, seasonal and interannual variation in biomass, 1994-1998. *Deep-Sea Research Part II-Topical Studies in Oceanography*, *48*(8–9), 2063–2082. https://doi.org/10.1016/s0967-0645(00)00171-5

Marsay, C. M., Sanders, R. J., Henson, S. A., Pabortsava, K., Achterberg, E. P., & Lampitt, R. S. (2015). Attenuation of sinking particulate organic carbon flux through the mesopelagic ocean. *Proceedings of the National Academy of Sciences of the United States of America*, *112*(4), 1089–1094. https://doi.org/10.1073/pnas.1415311112

Martin, A., Boyd, P., Buesseler, K., Cetinic, I., Claustre, H., Giering, S., et al. (2020). The oceans' twilight zone must be studied now, before it is too late. *Nature*, *580*(7801), 26–28. https://doi.org/10.1038/d41586-020-00915-7

McLaren, I. A. (1963). Effects of temperature on growth of zooplankton, and the adaptive value of vertical migration. *Journal of the Fisheries Research Board of Canada*, *20*(3), 685–727. https://doi.org/10.1139/f63-046

Meissner, K., Weaver, A., Matthews, H., & Cox, P. (2003). The role of land surface dynamics in glacial inception: A study with the Uvic Earth System Model. *Climate Dynamics*, *21*(7–8), 515–537. https://doi.org/10.1007/s00382-003-0352-2

Mitra, A., Castellani, C., Gentleman, W. C., Jónasdóttir, S. H., Flynn, K. J., Bode, A., et al. (2014). Bridging the gap between marine biogeochemical and fisheries sciences; configuring the zooplankton link. *Progress in Oceanography*, *129*, 176–199. https://doi.org/10.1016/j.pocean.2014.04.025

Mouw, C. B., Barnett, A., McKinley, G. A., Gloege, L., & Pilcher, D. (2016). Global ocean particulate organic carbon flux merged with satellite parameters. *Earth System Science Data*, *8*(2), 531–541. https://doi.org/10.5194/essd-8-531-2016

Myers, R., & Worm, B. (2003). Rapid worldwide depletion of predatory fish communities. *Nature*, *423*(6937), 280–283. https://doi.org/10.1038/nature01610

Nowicki, M., DeVries, T., & Siegel, D. A. (2022). Quantifying the carbon export and sequestration pathways of the ocean's biological carbon pump. *Global Biogeochemical Cycles*, *36*(3), e2021GB007083. https://doi.org/10.1029/2021GB007083

Olsen, R. E., Strand, E., Melle, W., Nørstebø, J. T., Lall, S. P., Ringø, E., et al. (2020). Can mesopelagic mixed layers be used as feed sources for salmon aquaculture? *Deep-Sea Research Part II*, *180*, 104722. https://doi.org/10.1016/j.dsr2.2019.104722

Oschlies, A., Brandt, P., Stramma, L., & Schmidtko, S. (2018). Drivers and mechanisms of ocean deoxygenation. *Nature Geoscience*, *11*(7), 467–473. https://doi.org/10.1038/s41561-018-0152-2

Pacanowski, R. C. (1995). *Mom 2 documentation user's guide and reference manual. Technical Report 3*. GFDL Ocean Group.

Paffenhöfer, G., & Strickland, J. (1970). A note on the feeding of calanus helgolandicus on detritus. *Marine Biology*, *5*(2), 97–99. https://doi.org/10.1007/bf00352591

Phillips, B., Kremer, P., & Madin, L. P. (2009). Defecation by salpa thompsoni and its contribution to vertical flux in the Southern Ocean. *Marine Biology*, *156*(3), 455–467. https://doi.org/10.1007/s00227-008-1099-4

Piccolin, F., Pitzschler, L., Biscontin, A., Kawaguchi, S., & Meyer, B. (1986). Circadian regulation of diel vertical migration (DVM) and metabolism in Antarctic krill *Euphausia superba*. *Scientific Reports*, *10*(1), 6671–6681. https://doi.org/10.1029/JD091iD06p06671

Pinti, J., DeVries, T., Norin, T., Serra-Pompei, C., Proud, R., Siegel, D. A., et al. (2023). Model estimates of metazoans' contributions to the biological carbon pump. *Biogeosciences*, *20*(5), 997–1009. https://doi.org/10.5194/bg-20-997-2023

Punt, A. E., Castillo-Jordán, C., Hamel, O. S., Cope, J. M., Maunder, M. N., & Ianelli, J. N. (2021). Consequences of error in natural mortality and its estimation in stock assessment models. *Fisheries Research*, *233*, 105759. https://doi.org/10.1016/j.fishres.2020.105759

Saba, G. K., Burd, A. B., Dunne, J. P., Hernández-León, S., Martin, A. H., Rose, K. A., et al. (2021). Toward a better understanding of fish-based contribution to ocean carbon flux. *Limnology & Oceanography*, *66*(5), 1639–1664. https://doi.org/10.1002/lno.11709

Saba, G. K., & Steinberg, D. K. (2012). Abundance, composition and sinking rates of fish fecal pellets in the Santa Barbara channel. *Scientific Reports*, *2*(1), 1639–1664. https://doi.org/10.1038/srep00716

Saunders, R. A., Hill, S. L., Tarling, G. A., & Murphy, E. J. (2019). Myctophid fish (family Myctophidae) are central consumers in the food web of the Scotia Sea (Southern Ocean). *Frontiers in Marine Science*, *6*. https://doi.org/10.3389/fmars.2019.00530

Schmidtko, S., Stramma, L., & Visbeck, M. (2017). Decline in global oceanic oxygen content during the past five decades. *Nature*, *542*(7641), 335–339. https://doi.org/10.1038/nature21399

Simmons, H. L., Jayne, S. R., Laurent, L. C., & Weaver, A. J. (2004). Tidally driven mixing in a numerical model of the ocean general circulation. *Ocean Modelling*, *6*(3), 245–263. https://doi.org/10.1016/S1463-5003(03)00011-8

Staresinic, N., Farrington, J., Gagosian, R. B., Clifford, C. H., & Hulburt, E. M. (1983). Downward transport of particulate matter in the Peru coastal upwelling: Role of the anchoveta, Engraulis ringens. In E. Suess, & J. Thiede (Eds.), *Coastal upwelling its sediment record: Part A: Responses of the sedimentary regime to present coastal upwelling* (pp. 225–240). https://doi.org/10.1007/978-1-4615-6651-9_12

Steele, J., & Henderson, E. (1992). The role of predation in plankton models. *Journal of Plankton Research*, *14*(1), 157–172. https://doi.org/10.1029/97JC03198

Steinberg, D. K., Carlson, C. A., Bates, N. R., Goldthwait, S. A., Madin, L. P., & Michaels, A. F. (2000). Zooplankton vertical migration and the active transport of dissolved organic and inorganic carbon in the Sargasso Sea. *Deep Sea Research Part I: Oceanographic Research Papers*, *47*(1), 137–158. https://doi.org/10.1016/S0967-0637(99)00052-7

Steinberg, D. K., Cope, J. S., Wilson, S. E., & Kobari, T. (2008). A comparison of mesopelagic mesozooplankton community structure in the subtropical and subarctic North Pacific Ocean. *Deep Sea Research Part II: Topical Studies in Oceanography*, *55*(14–15), 1615–1635. https://doi.org/10.1016/j.dsr2.2008.04.025

Steinberg, D. K., Stamieszkin, K., Maas, A. E., Durkin, C. A., Passow, U., Estapa, M. L., et al. (2023). The outsized role of salps in carbon export in the subarctic northeast Pacific Ocean. *Global Biogeochemical Cycles*, *37*(1), e2022GB007523. https://doi.org/10.1029/2022GB007523

Steinberg, D. K., Van Mooy, B. A. S., Buesseler, K. O., Boyd, P. W., Kobari, T., & Karl, D. M. (2008). Bacterial vs. zooplankton control of sinking particle flux in the ocean's twilight zone. *Limnology & Oceanography*, *53*(4), 1327–1338. https://doi.org/10.4319/lo.2008.53.4.1327

St. John, M. A., Borja, A., Chust, G., Heath, M., Grigorov, I., Mariani, P., et al. (2016). A dark hole in our understanding of marine ecosystems and their services: Perspectives from the mesopelagic community. *Frontiers in Marine Science*, *3*. https://doi.org/10.3389/fmars.2016.00031

Then, A. Y., Hoenig, J. M., Hall, N. G., & Hewitt, D. A. A. (2014). Evaluating the predictive performance of empirical estimators of natural mortality rate using information on over 200 fish species. *ICES Journal of Marine Science*, *72*(1), 82–92. https://doi.org/10.1093/icesjms/fsu136

Tönnesson, K., & Tiselius, P. (2005). Diet of the chaetognaths Sagitta setosa and S. elegans in relation to prey abundance and vertical distribution. *Marine Ecology Progress Series*, *289*, 177–190. https://doi.org/10.3354/meps289177

Turner, J. T. (2015). Zooplankton fecal pellets, marine snow, phytodetritus and the ocean's biological pump. *Progress in Oceanography*, *130*, 205–248. https://doi.org/10.1016/j.pocean.2014.08.005

Wang, F., Wu, Y., Chen, Z., Zhang, G., Zhang, J., Zheng, S., & Kattner, G. (2019). Trophic interactions of mesopelagic fishes in the South China Sea illustrated by stable isotopes and fatty acids. *Frontiers in Marine Science*, *5*. https://doi.org/10.3389/fmars.2018.00522

Weaver, A. J., Eby, M., Wiebe, E. C., Bitz, C. M., Duffy, P. B., Ewen, T. L., et al. (2001). The UVic Earth system climate model: Model description, climatology, and applications to past, present and future climates. *Atmosphere-Ocean*, *39*(4), 361–428. https://doi.org/10.1080/07055900.2001.9649686

Westberry, T., Behrenfeld, M. J., Siegel, D. A., & Boss, E. (2008). Carbon-based primary productivity modeling with vertically resolved photoacclimation. *Global Biogeochemical Cycles*, *22*(2). https://doi.org/10.1029/2007GB003078

Yang, G., Atkinson, A., Pakhomov, E. A., Hill, S. L., & Racault, M.-F. (2022). Massive circumpolar biomass of Southern Ocean zooplankton: Implications for food web structure, carbon export, and marine spatial planning. *Limnology & Oceanography*, *67*(11), 2516–2530. https://doi.org/10.1002/lno.12219

Zhang, X., & Dam, H. G. (1997). Downward export of carbon by diel migrant mesozooplankton in the central equatorial Pacific. *Deep Sea Research Part II: Topical Studies in Oceanography*, *44*(9–10), 2191–2202. https://doi.org/10.1016/S0967-0645(97)00060-X